Journal of Medicinal Chemistry

ARTICLE

pubs.acs.org/jmc

Synthesis, In Vivo Occupancy, and Radiolabeling of Potent Phosphodiesterase Subtype-10 Inhibitors as Candidates for Positron Emission Tomography Imaging

José-Ignacio Andrés,*[,†] Meri De Angelis,[†] Jesús Alcázar,[†] Laura Iturrino,[†] Xavier Langlois,[‡] Stefanie Dedeurwaerdere,[‡] Ilse Lenaerts,[‡] Greet Vanhoof,[‡] Sofie Celen,[§] and Guy Bormans[§]

[†]Medicinal Chemistry, Janssen Research & Development, Janssen-Cilag SA, C/Jarama 75, 45007 Toledo, Spain

[‡]Neuroscience, Janssen Research & Development, Janssen Pharmaceutica NV, Turnhoutseweg 30, B-2340 Beerse, Belgium

[§]Laboratory for Radiopharmacy and IMIR, Faculty of Pharmaceutical Sciences, KU Leuven, Herestraat 49, B-3000 Leuven, Belgium

Supporting Information

ABSTRACT: We have recently reported the phosphodiesterase 10A (PDE10A) inhibitor 2-[4-[1-(2-[^{18}F]fluoroethyl)-4-pyridin-4-yl-1*H*-pyrazol-3-yl]-phenoxymethyl]-quinoline ([^{18}F]**1a**) as a promising candidate for in vivo imaging using positron emission tomography (PET). We now describe the synthesis and biological evaluation of a series of related pyridinyl analogues that exhibit high potency and selectivity as PDE10A inhibitors. The most interesting compounds were injected in rats to measure their levels of PDE10A occupancy through an in vivo occupancy assay. The 3,5-dimethylpyridine derivative **3** and the 5-methoxypyridine derivative **4** showed a comparable level of occupancy to that of **1a**. Because these derivatives showed lower in vitro activity and are slightly less lipophilic than **1a**, we hypothesized that they could behave as better PET imaging ligands. Compounds [^{18}F]**3**, [^{18}F]**4**, and [^{11}C]**4** were radiosynthesized and subjected to biodistribution studies in rats for a preliminary evaluation as candidate PET radioligands for in vivo imaging of PDE10A in the brain.

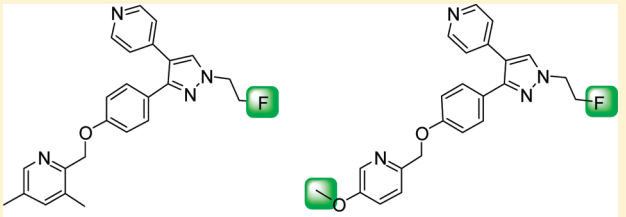

PDE10A inhibitors as potential PET ligands

INTRODUCTION

Phosphodiesterases (PDEs) are a family of enzymes encoded by 21 genes and subdivided into 11 distinct families according to structural and functional properties. These enzymes metabolically inactivate widely occurring intracellular secondary messengers, 3′,5′-cyclic adenosine monophosphate (cAMP) and 3′,5′-cyclic guanosine monophosphate (cGMP).[1] These two messengers regulate a wide variety of biological processes, including pro-inflammatory mediator production and action, ion channel function, muscle contraction, learning, differentiation, apoptosis, lipogenesis, glycogenolysis, and gluconeogenesis. They do this by activation of cAMP or cGMP dependent kinases, respectively, protein kinase A (PKA) and protein kinase G (PKG), which in turn phosphorylate a wide variety of substrates including transcription factors and ion channels that regulate innumerable physiological responses. In neurons, this includes phosphorylation of proteins involved in acute regulation of synaptic transmission as well as in neuronal differentiation and survival.[2] The discovery of PDE10A was reported in 1999.[3] Of all 11 known PDE families, PDE10A has the most restricted distribution with high mRNA expression only in the brain and testes. In brain, PDE10A mRNA and protein are highly expressed in the medium spiny neurons of the striatum.[4,5] This unique distribution of PDE10A in the brain, together with its pharmacological characterization, points to the potential use of PDE10A inhibitors for treating neurological and psychiatric disorders like schizophrenia.[6]

Noninvasive imaging of PDE10A using PET would allow for studying the distribution of this enzyme in vivo in these diseases. Furthermore, it would be useful for clinical development of PDE10A inhibitors as potential antipsychotic drugs by giving direct insight into the relationship between the occupancy and the administered dose of the candidate drug.[7,8]

The first reported attempt to visualize PDE10A has recently been made by Tu and co-workers, who successfully radiolabeled the in vitro relatively selective PDE10A inhibitor papaverine with carbon-11 ([^{11}C]**2**, Chart 1). Unfortunately this ligand failed as a PET tracer due to rapid washout of the tracer from striatum, as was observed in rat biodistribution studies and small-animal PET brain imaging in monkey.[9] We have reported the in vivo evaluation of the new PDE10A PET radiotracer 2-[4-[1-(2-[^{18}F]-fluoroethyl)-4-pyridin-4-yl-1*H*-pyrazol-3-yl]-phenoxymethyl]-quinoline ([^{18}F]**1a**),[10] an analogue of the potent PDE10A inhibitor MP-10 (**1b**, 2-[4-(1-methyl-4-pyridin-4-yl-1*H*-pyrazol-3-yl)-phenoxymethyl]-quinoline)[11] (Chart 1). Biodistribution studies and small-animal PET in rats and PDE10A knockout mice

Received: April 30, 2011
Published: July 22, 2011

Chart 1. Structures of Some PDE10A Inhibitors and Derived PET Radioligands

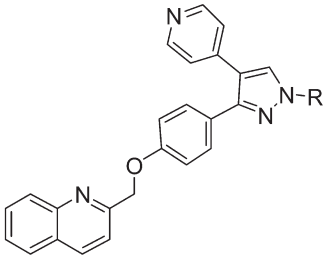

[^{18}F]**1a**, R = CH_2-CH_2-^{18}F
1b, MP-10, R = CH_3
[^{11}C]**1b**, [^{11}C]MP-10, R = $^{11}CH_3$

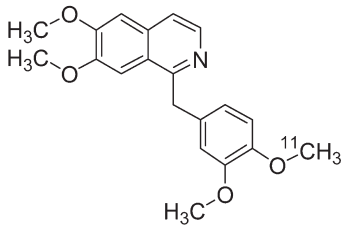

2, [^{11}C]papaverine

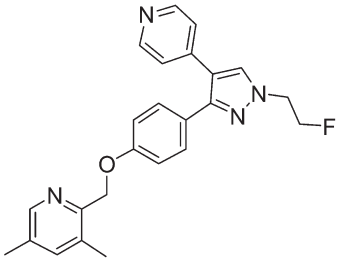

3

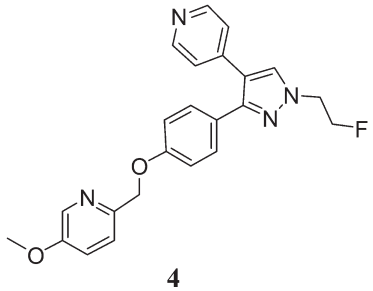

4

demonstrated that [^{18}F]**1a** shows specific and reversible binding to PDE10A in striatum.[10] [^{18}F]**1a** is, to our knowledge, the first successful PDE10A PET imaging tracer reported so far. A possible drawback of this radioligand could be its relatively high lipophilicity and associated high plasma protein binding (99.5% both in humans and rats).[12] Despite our very encouraging preliminary results, it was also found that this radiotracer showed relatively slow kinetics, which may require longer acquisition times in clinical application to obtain robust distribution volume values.[10] This behavior could be related to the high level of potency of compound **1a** (pIC_{50} = 9.3). In fact, it is known from literature that increased affinity is associated with slower binding kinetics, thus requiring longer scanning time. Thus, the affinity of a radiotracer should always represent a compromise between the need to measure high signal-to-noise ratio and the need to have fast binding kinetics that match the relatively short image acquisition window imposed by the short half-life of carbon-11 (20 min) and fluorine-18 (110 min).[13] Recently, our group[14] and Tu et al. independently reported the evaluation of [^{11}C]MP-10 ([^{11}C]**1b**) as potential PDE10A PET ligand. Tu et al. concluded that the presence of a radiolabeled metabolite capable of penetrating the blood−brain barrier may limit the clinical utility of [^{11}C]**1b** as a PDE10A PET tracer.[15]

In view of the SAR around this chemical series, it could be anticipated that the replacement of the quinoline moiety with monocyclic heteroaromatic rings, such as for example substituted pyridines, would lead to significantly less potent PDE10A inhibitors.[11,16] However, although the potency of the monocyclic analogues would be decreased, having in mind the extremely high inhibitory activity of **1a**, we might still identify derivatives with sufficient potency but more optimal lipophilicity, resulting in PET tracers showing a faster kinetic profile. Therefore, we decided to initiate a chemical exploration around compound **1a**, in which the 2-quinolinyl heterocycle was replaced by differently substituted 2-pyridinyl moieties. Thus, the aims of this investigation were (i) to synthesize close analogues of **1a** that can be easily radiolabeled with either ^{11}C or ^{18}F, (ii) to determine their in vitro PDE10A potency and selectivity, (iii) to measure the in vivo brain occupancy of the most promising derivatives, and (iv) to radiolabel the potential candidates with ^{18}F or ^{11}C to further assess their suitability as PDE10A PET imaging agents in vivo.

RESULTS AND DISCUSSION

Chemistry and Radiochemistry. The synthesis of the final compounds is outlined in Schemes 1 and 2. Derivatives **6a** and **6b** were obtained starting from the common intermediate **5**, whose synthesis is described in literature,[17] by an alkylation reaction either with trifluoroethyl iodide or with 1-fluoro-2-bromoethane. Product **6c** was synthesized by a Mitsunobu type reaction using 3-fluoro-1-propanol as alkylating agent. Those reactions afforded mixtures of the two possible regioisomers **6a**−**c** and **7a**−**c** that were separated by column chromatography. Subsequently the desired derivatives **6a**−**c** were subjected to debenzylation by hydrogenation in a H-cube apparatus, affording intermediate compounds **8a**−**c**. These derivatives were coupled with different 2-hydroxymethylpyridines, either commercially available or synthesized following methodologies described in literature (see Experimental Section), by a Mitsunobu type reaction yielding the final products **3**, **4**, **9**−**12**, and **15**−**28** (Scheme 1). Compounds **13** and **14** were both synthesized starting from compound **12**. Thus, **13** was obtained by a copper catalyzed reaction using a sort of fluorosulfonylfluoroacetate reagent as a precursor for the in situ generation of trifluoromethide species,[18] whereas compound **14** was obtained by a Suzuki coupling reaction using cyclopropylboronic acid (Scheme 2). The final compounds were

dx.doi.org/10.1021/jm200536d |*J. Med. Chem.* 2011, 54, 5820–5835

Scheme 1. Synthesis of final compounds 3, 4, 9−12, and 15−28[a]

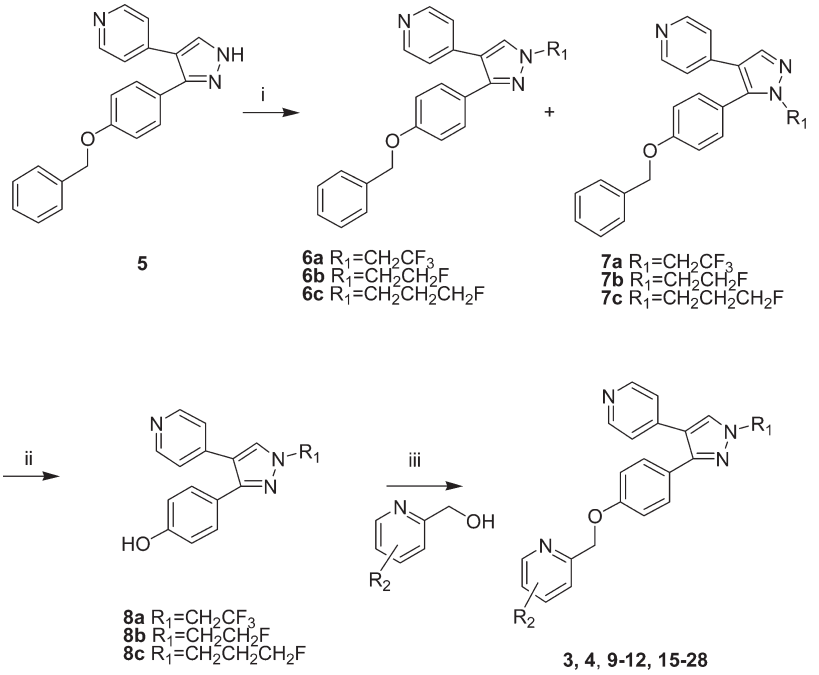

[a] Reagents and conditions: (i) Cs_2CO_3, ICH_2CF_3 ($R_1 = CH_2CF_3$), DMF, MW, 120 °C, 20 min, or Cs_2CO_3, FCH_2CH_2Br ($R_1 = CH_2CH_2F$), DMF, MW, 120 °C, 20 min, or DIAD, PPh_3, $F(CH_2)_3OH$ ($R_1 = (CH_2)_3F$), THF, MW, 120° C, 20 min, 27−52%; (ii) 5% Pd−C, H_2, 1 atm, EtOH, 80 °C, 75−82%; (iii) DIAD, PPh_3, THF, MW, 120 °C, 20 min, 16−86%.

Scheme 2. Synthesis of Final Compounds 13 and 14 from 12[a]

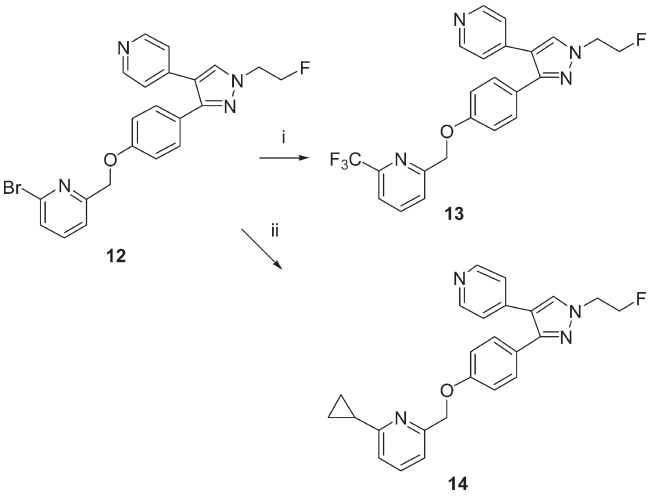

[a] Reagents and conditions: (i) methyl-2,2-difluoro-2-(fluorosulfonyl)-acetate, CuI, DMF, 120 °C, 2 h, 7%; (ii) $Pd(PPh_3)_4$, cyclopropylboronic acid, aq Na_2CO_3/1,4-dioxane, MW, 130 °C, 15 min, 54%.

isolated either as free bases or as hydrochloric or succinic acid salts.

In view of the in vitro and in vivo pharmacological results (see Pharmacology section) compounds **3** and **4** were selected as potential PET radioligands for imaging of PDE10A. In a first attempt, the synthesis of the required precursor and its radiolabeling to obtain [^{18}F]**3** were performed as described in Scheme 3. Thus, the Mitsunobu type reaction between 4-hydroxybenzoic acid methyl ester (**29**) and 3,5-dimethyl-2-hydroxymethylpyridine yielded intermediate **30**, which was easily converted into the Weinreb amide **31** through a described procedure.[11] Further reaction with the anion of 4-picoline formed with lithium diisopropyl amide (LDA) afforded compound **32**. Subsequent treatment of this intermediate with dimethoxymethyl-dimethyl amine to form the enaminone followed by addition of hydrazine gave the desired pyrazole precursor **33**. This compound was then radiolabeled using the secondary labeling agent [^{18}F]fluoroethyl bromide ([^{18}F]FEtBr) to give a mixture of radiolabeled regioisomers [^{18}F]**3** and [^{18}F]**34** (Scheme 3), which could be separated by semipreparative reversed phase HPLC (RP-HPLC) using a mixture of ethanol and an acidic phosphate buffer. [^{18}F]-FEtBr was synthesized following a reported procedure with some modifications.[19] The radiochemical yield relative to starting radioactivity of [^{18}F]FEtBr was 45% ([^{18}F]**3**) and 22% ([^{18}F]**34**). After purification and formulation [^{18}F]**3**, the desired regioisomer was analyzed on an analytical C_{18} column and its radiochemical purity was found to be more than 98%. We also developed an alternative method to produce [^{18}F]**3** via direct labeling of the *O*-mesyl-precursor starting from [^{18}F]fluoride. Alkylation of **33** with methyl bromoacetate followed by reduction of the carboxyl groups with sodium borohydride led to the mixture of regioisomers **35a** and **35b** (Scheme 4), which were separated by column chromatography. The hydroxyl group of the desired isomer **35a** was converted into the corresponding mesylate derivative using methane sulfonic anhydride to allow direct nucleophilic substitution with free [^{18}F]fluoride (Scheme 4). To reduce the number of synthetic steps, a direct alkylation of pyrazole **33** using 2-bromo-1-ethanol was tried, but the yield of the hydroxyl intermediates **35a**−**b** was quite low although different reaction conditions were tested. Unluckily, the mesyl intermediate of **35a**

Scheme 3. Synthesis of Precursor 33 and Subsequent Radiosynthesis of [^{18}F]3[a]

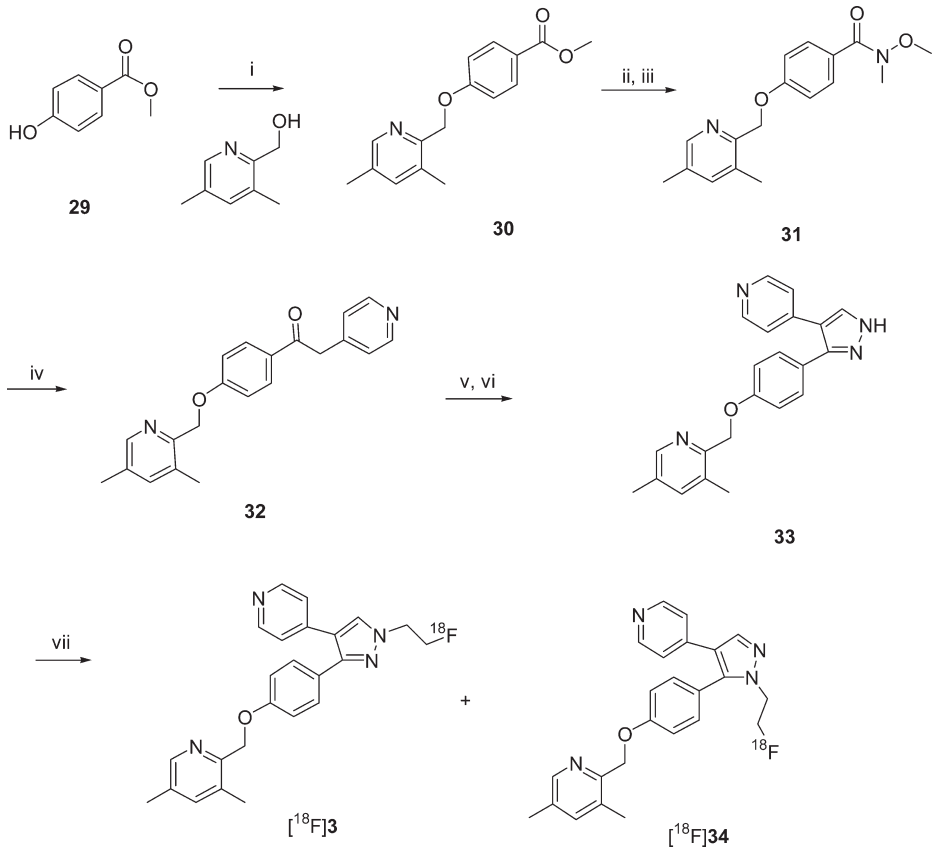

[a] Reagents and conditions: (i) DIAD, PPh_3, THF, MW, 120 °C, 20 min, 84%; (ii) NaOH, MeOH−THF, rt, 18 h; (iii) $SOCl_2$, rt, 3 h, then Et_3N, NHMeOMe, THF, rt, 18 h, 54% (2 steps); (iv) 4-picoline, LDA −78 °C, 30 min, 71%; (v) dimethylformamide−dimethylacetal, reflux, 1 h; (vi) NH_2NH_2, MeOH, reflux, 1 h, 36% (2 steps); (vii) [^{18}F]FCH_2CH_2Br, Cs_2CO_3, DMF, 90 °C, 15 min, 45% RCY.

Scheme 4. Synthesis of Precursor 35a and Subsequent Radiosynthesis of [^{18}F]3[a]

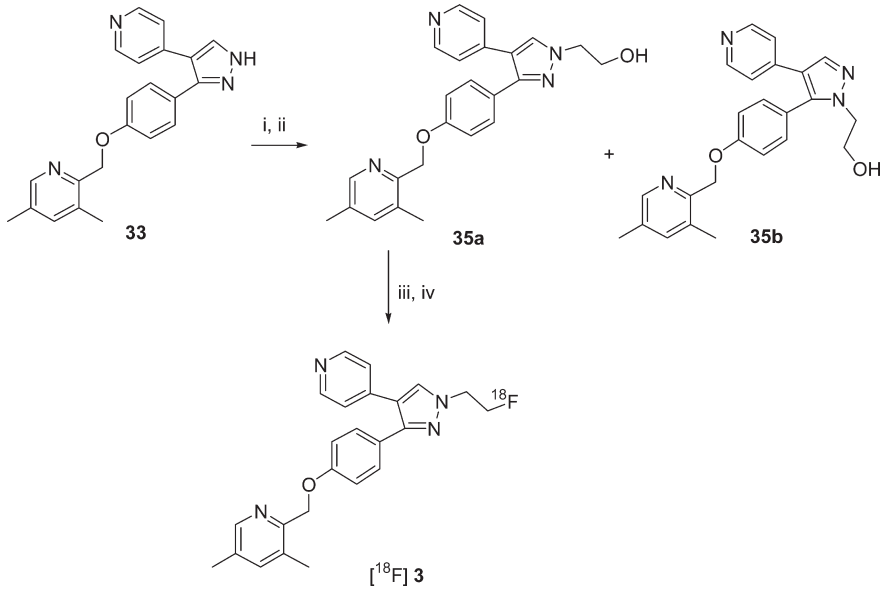

[a] Reagents and conditions: (i) Cs_2CO_3, methyl bromoacetate, DMF, rt, 3 h; (ii) $NaBH_4$, MeOH/DCM, rt, 1 h, 28% (2 steps); (iii) methanesulfonic anhydride, pyridine, DCM, 0 °C, 4 h; (iv) [^{18}F]F^-/K_2CO_3/Kryptofix-[2.2.2], DMF, 90 °C, 15 min, 17% RCY.

dx.doi.org/10.1021/jm200536d |J. Med. Chem. 2011, 54, 5820–5835

Scheme 5. Synthesis of Precursor 37 and Subsequent Radiosynthesis of [^{11}C]4[a]

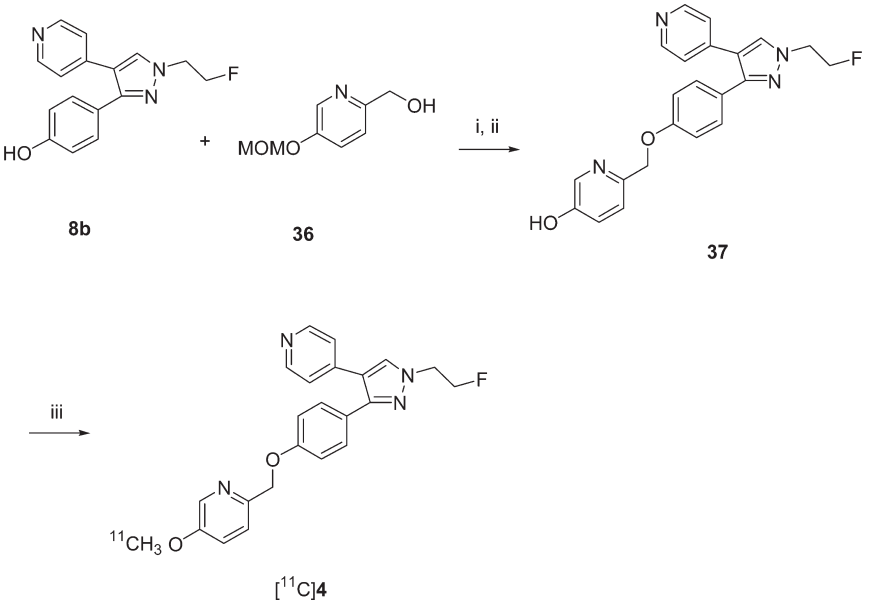

[a] Reagents and conditions: (i) DIAD, PPh_3, THF, MW, 120 °C, 20 min; (ii) TFA, DCM, rt, 24 h, 70% (2 steps); (iii) [^{11}C]CH_3OTf, Cs_2CO_3, DMF, RT, 5 min, <15% RCY.

(radiolabeling precursor) was found to be rather unstable over time, although it could be isolated. To reach an acceptable radiochemical yield, preparation of the mesylate derivative of **35a** as precursor for radiolabeling was done in situ on the day before the radiolabeling. Introduction of the ^{18}F-label, a nucleophilic substitution of a [^{18}F]fluoride atom for the *O*-mesyl leaving group, was achieved by heating the solution of the mesylate precursor with K[^{18}F]F-kryptofix complex in DMF at 90 °C for 15 min. The crude radiolabeling mixture was purified using semipreparative RP-HPLC, affording [^{18}F]**3** in a 17% radiochemical yield (relative to starting radioactivity of [^{18}F]F^-). The radiochemical purity of [^{18}F]**3** examined onto an analytical C_{18} column was more than 97%.

Because compound **4** was amenable to radiolabeling both with ^{11}C and ^{18}F, two different radiolabeling precursors were synthesized. Starting from intermediate **8b** and 5-(methoxy-ethoxymethoxy)-2-hydroxymethylpyridine **36**,[20] precursor **37** was easily obtained through a Mitsunobu type reaction, followed by the removal of the protecting MOM group (Scheme 5). Radiolabeling of compound **37** with ^{11}C was troublesome. Heating in the presence of a soft base (Cs_2CO_3) resulted in degradation of the precursor. When heating was applied in the absence of base, no reaction product was formed even when the more reactive [^{11}C]methyltriflate ([^{11}C]MeOTf) was used. At room temperature with Cs_2CO_3 in DMF, the precursor could be alkylated using [^{11}C]MeOTf (Scheme 5), however the yield of [^{11}C]**4** was very low (<15%). Because the synthesis of [^{18}F]**4** was more successful, the ^{18}F-labeled derivative of **4** was further evaluated in vivo in rats. No further efforts were made to improve the production of [^{11}C]**4**. The synthesis of the radiolabeling precursor for production of [^{18}F]**4** was achieved starting from derivative **38**[11] (Scheme 6). Alkylation with methyl bromoacetate afforded a mixture of isomers **39a**−**b**. Hydrogenation was applied to remove the quinoline groups, which were subsequently replaced with 5-methoxy-2-hydroxylpyridine by a Mitsunobu reaction. After reduction of the carboxyl groups, the corresponding hydroxyl intermediates **40a**−**b** were obtained and could be separated by column chromatography. Finally, precursor **40a** was converted into the mesyl derivative, which was radiolabeled with [^{18}F]F^- using a similar procedure as that applied for production of [^{18}F]**3** and was purified by RP-HPLC. [^{18}F]**4** was obtained with an overall decay corrected radiochemical yield (RCY) of 18% and a radiochemical purity >99%.

Pharmacology. The in vitro inhibitory activity against PDE10A enzyme was evaluated for all final compounds (see Experimental Section). As it could be anticipated, these new pyridinyl derivatives were less potent than their quinolinyl counterparts,[11,16] however, they still exhibited significant PDE10A inhibition potency. Furthermore, some of them showed indeed very high activity ranging from pIC_{50} = 7.0 to 8.8 (Table 1). For this study, we focused our exploration on two parts of the molecule: substitution on the pyrazole ring with three different fluoroalkyl chains (fluoroethyl, fluoropropyl, and trifluoroethyl) and different substitution patterns on the pyridinyl moiety taking into account the commercial availability of starting materials. In our first approach, we aimed to find the most appropriate alkyl chain on the pyrazole ring. We found that substitution with fluoroethyl and trifluoroethyl moieties showed comparable potency, whereas corresponding analogues with the fluoropropyl substituent were less active (Table 1: compare compounds **4** and **11** vs **17**; **18** and **15** vs **16**; **9** vs **10**). Having in mind that the fluoroethyl chain would be a very accessible point for radiolabeling with ^{18}F, we investigated the effect of different substitution patterns in the pyridinyl ring against the inhibitory activity, keeping the fluoroethyl substituent fixed on the pyrazole ring. In general, compounds with a methoxy group in either position of the pyridinyl ring, such as **4**, **18**, and **24**, were very potent, with pIC_{50} values around 8.5. However, when this group was replaced by several other substituents such as halogen (**12**, **19**, and **20**), trifluoromethyl (**13** and **22**), cyano (**21** and **26**), cyclopropyl (**14** and **23**), or ethoxy (**25**), a

Scheme 6. Synthesis of Precursor 40a and Subsequent Radiosynthesis of [^{18}F]4[a]

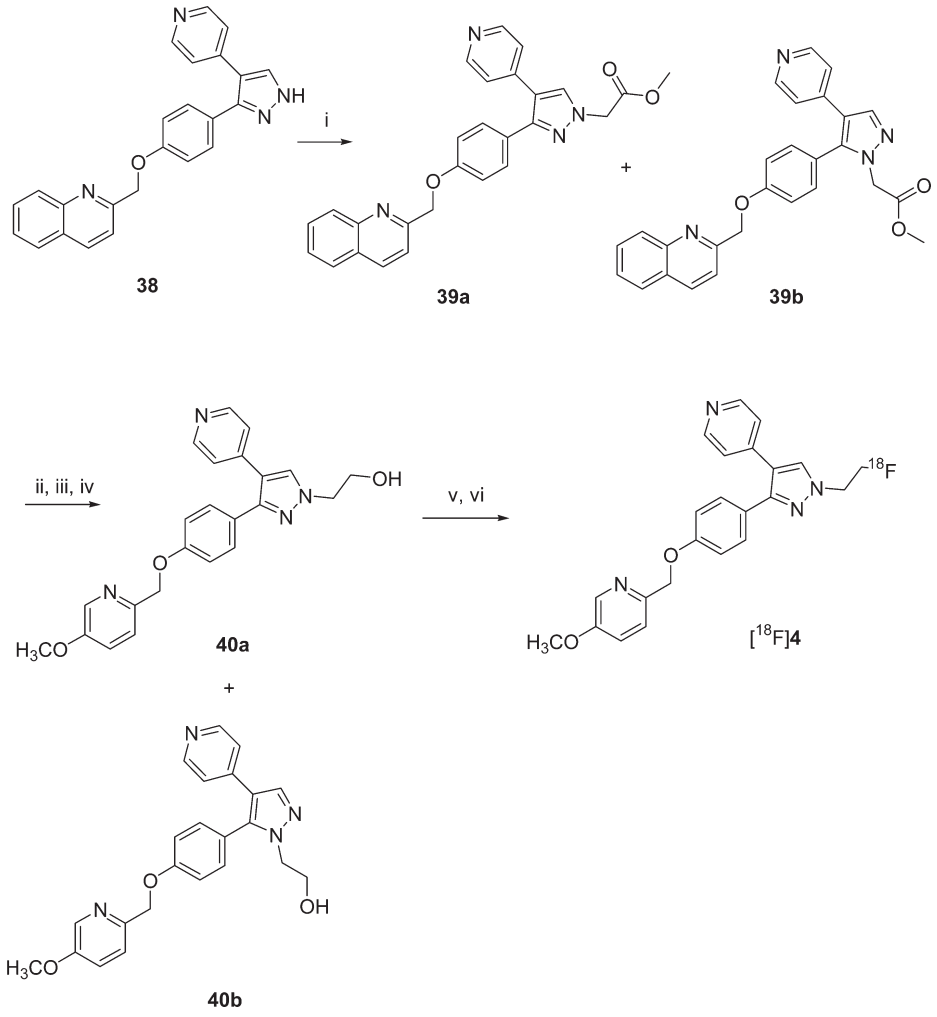

[a] Reagents and conditions: (i) Cs_2CO_3, methyl bromoacetate, DMF, rt, 3 h, 47%; (ii) 10% Pd−C, H_2, 1 atm, EtOH, 70 °C, 67%; (iii) DIAD, PPh_3, 5-methoxy-2-(hydroxymethyl)pyridine, THF, MW,120 °C, 20 min; (iv) $NaBH_4$, MeOH/DCM, rt, 3 h, 53% (2 steps); (v) methanesulfonic anhydride, pyridine, DCM, 0 °C, 4 h; (vi) [^{18}F]F^-/K_2CO_3/Kryptofix-[2.2.2], DMF, 90 °C, 15 min, 18% RCY.

significant drop in activity was observed, being in some cases more than one log unit. Substitution with a methyl group on the pyridinyl ring, as was the case for the 6-methylpyridinyl derivative **9** and the dimethyl and trimethyl derivatives **3** and **28**, led to the most potent compounds of this series with a pIC_{50} = 8.8 for **3**, pIC_{50} = 8.6 for **9**, and pIC_{50} = 8.4 for **28**. One might argue that higher PDE10A inhibition could be linked to a higher lipophilicity in the pyridinyl pocket, but the calculated lipophilicity (clogP)[21] of the compounds (Table 1) does not support this hypothesis. It is known that clogP values can be useful for predicting the relative ability of ligands to pass the blood−brain barrier.[13,22] Moderate lipophilicity, in the clogP range of 2.5−3.5, is normally considered as optimal for adequate brain penetration without an excessive level of nonspecific binding. The most active compounds listed in Table 1 showed clogP values around 3.5 that fit within the acceptable range and are more favorable than that of compound **1a** (Table 1) in terms of nonspecific binding as well as of plasma protein binding .

The inhibitory activity against a panel of different PDE iso enzymes of the most potent compounds was also assessed. The selectivity over other PDEs was in all cases >50-fold and for most of the compounds >100-fold (unpublished results). The most promising compounds were also evaluated in an in vivo occupancy assay to ascertain their ability to enter the brain and to bind specifically to the enzyme. For this purpose, the selective PDE10A inhibitor **1b** in its tritiated version was used as radiotracer for the study. Membrane homogenate binding and autoradiography experiments in rat brain have demonstrated that [^{3}H]**1b** is a high affinity and selective PDE10A radioligand.[23] In addition, its high brain uptake and low level of nonspecific binding make it an excellent radioligand for measuring PDE10A occupancy by drug candidates. As shown in Figure 1 and Table 2, compound **1a**, which is an established PDE10 PET radioligand, is one of the most potent compounds to occupy the enzyme. This result indicates that other compounds showing similar potencies in the occupancy assay would deserve to be radiolabeled and tested as potential PDE10A PET tracers. It is noteworthy that several compounds tested in this in vivo occupancy assay showed brain penetration, although with quite different ED_{50} values after subcutaneous administration (Table 2 and Figure 1). The most

dx.doi.org/10.1021/jm200536d |J. Med. Chem. 2011, 54, 5820–5835

Table 1. In Vitro PDE10A Inhibitory Activity and Calculated clogP Values of Final Compounds

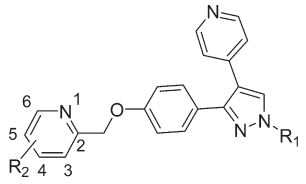

compd	R_1	R_2	pIC_{50}[a]	clogP[b]
1b	CH_2CH_2F	(2-quinolinyl)	9.3	4.19
3	CH_2CH_2F	3,5-dimethyl	8.8	3.66
4	CH_2CH_2F	5-methoxy	8.5	3.13
9	CH_2CH_2F	6-methyl	8.6	3.21
10	$CH_2CH_2CH_2F$	6-methyl	7.7	3.44
11	CH_2CF_3	5-methoxy	8.3	3.17
12	CH_2CH_2F	6-bromo	8.0	3.66
13	CH_2CH_2F	6-trifluoromethyl	7.0	3.74
14	CH_2CH_2F	6-cyclopropyl	7.5	3.65
15	CH_2CF_3	3-methoxy	8.3	3.17
16	$CH_2CH_2CH_2F$	3-methoxy	7.9	3.36
17	$CH_2CH_2CH_2F$	5-methoxy	7.8	3.36
18	CH_2CH_2F	3-methoxy	8.4	3.13
19	CH_2CH_2F	3-fluoro	7.8	2.94
20	CH_2CH_2F	5-bromo	8.0	3.66
21	CH_2CH_2F	5-cyano	7.1	2.34
22	CH_2CH_2F	5-trifluoromethyl	7.0	3.74
23	CH_2CH_2F	5-cyclopropyl	7.5	3.65
24	CH_2CH_2F	6-methoxy	8.5	3.53
25	CH_2CH_2F	6-ethoxy	7.7	4.06
26	CH_2CH_2F	6-cyano	7.5	2.54
27	CH_2CH_2F	3-bromo-6-methoxy	7.5	4.43
28	CH_2CH_2F	3,4,5-trimethyl	8.4	4.06

[a] Values are mean of at least two experiments; a difference in pIC_{50} up to 0.6 (SD <0.5) was considered as reproducible and therefore accepted. [b] See ref 21.

promising compounds proved to be **3** and **4**, with ED_{50} = 0.46 mg/kg and ED_{50} = 1.3 mg/kg, respectively. Interestingly enough, these two compounds exhibited comparable occupancy to compound **1a** (ED_{50} = 0.48 mg/kg), although their in vitro activity was lower. Taking into account that the test compounds in this in vivo assay were administered subcutaneously, hence avoiding first-pass metabolism, it might be assumed that the observed occupancy would come from the parent compound and not, in part or completely, from active metabolites. However, we decided to identify the main metabolites formed from compounds **3** and **4** after incubation with human and rat liver microsomes.[24] The major metabolite route in both species for each compound was the loss of the differently substituted pyridinyl-2-methyl moieties, yielding the common phenolic intermediate **8b**. Several other different minor metabolites were also identified. Compound **8b** was screened as PDE10A inhibitor and, as expected from the knowledge within this chemical series, it was not active (pIC_{50} < 5). Therefore, we can conclude that active metabolites do not play a significant role in the observed in vivo occupancy results. Compounds **3** and **4** were also screened for affinity at a panel of other brain receptors, binding sites, and ion

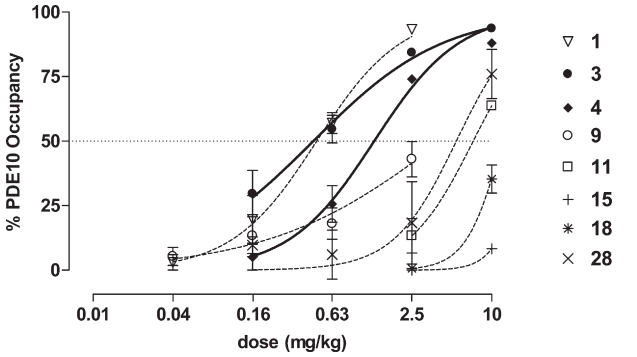

Figure 1. Dose-dependent occupancy of PDE10A in rat brain by different PDE10A inhibitors after sc administration using the radioligand [^{3}H]MP-10. Experimental details of the in vivo occupancy protocol are described in the Experimental Section. Bold curves highlight the two compounds (**3** and **4**) that were selected for radiolabeling and further investigation as potential PET ligands.

Table 2. In Vivo Occupancy of PDE10A in Rat Brain by Some Selected PDE10A Inhibitors after sc Administration Using the Radioligand [^{3}H]MP-10

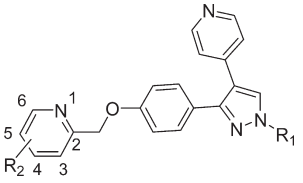

compd	R_1	R_2	ED_{50} (mg/kg)[a]
1a	CH_2CH_2F	(2-quinolinyl)	0.48
3	CH_2CH_2F	3,5-dimethyl	0.46
4	CH_2CH_2F	5-methoxy	1.3
9	CH_2CH_2F	6-methyl	>2.5
11	CH_2CF_3	5-methoxy	7.3
15	CH_2CF_3	3-methoxy	>10
18	CH_2CH_2F	3-methoxy	>10
28	CH_2CH_2F	3,4,5-trimethyl	5.4

[a] Experimental details of the in vivo occupancy protocol are described in the Experimental Section.

channels (CEREP, see Supporting Information). They did not show significant affinity for any of the screened targets except some dopamine transporter (DAT) inhibition (69% and 92% at 10^{-5} M, respectively). Both compounds were then tested in-house to obtain their DAT IC_{50} values, which resulted to be 2800 nM for **3** and 870 nM for **4**. These in vitro results proved that both derivatives were selective enough for in vivo imaging of PDE10A in the brain. They also showed, compared to **1a**, a much more favorable lipophilicity (clogP's = 3.66 for **3** and 3.16 for **4** vs 4.19 for **1a**). Our first successful PDE10A PET tracer [^{18}F]**1a** had a rather high lipophilicity and high potency and showed relatively slow kinetics, requiring longer acquisition times in clinical application to obtain robust distribution volume values.[10] Therefore, derivatives **3** and **4**, with their similar in vivo occupancy and lower lipophilicity as well as lower in vitro activity compared to **1a**, could be excellent PET ligand candidates which may have a more favorable kinetic profile than that of [^{18}F]**1a**.

Table 3. Radioactivity Brain Uptake upon Dosing of [^{18}F]3, [^{18}F]4, and [^{18}F]1a in Normal Rats

	%ID[a] at 2 min pi		
	[^{18}F]**3**	[^{18}F]**4**	[^{18}F]**1a**
total brain	0.368 ± 0.068	0.400 ± 0.017	0.565 ± 0.004
cerebrum	0.305 ± 0.049	0.317 ± 0.014	0.447 ± 0.009
cerebellum	0.071 ± 0.016	0.065 ± 0.011	0.101 ± 0.015

[a] Percentage of injected dose calculated as cpm in organ/total cpm recovered. Data are expressed as mean ± SD; n = 3 per time point.

Table 4. Radioactivity in Different Rat Brain Regions and Blood at 2, 30, and 60 min upon Dosing of [^{18}F]3 and [^{18}F]4

	SUV[a]				
	[^{18}F]**3**			[^{18}F]**4**[b]	
	2 min	30 min	60 min	2 min	30 min
sttriatum	1.0 ± 0.1	1.2 ± 0.2	1.8 ± 0.5	2.3 ± 0.1	1.3 ± 0.1
hippocampus	0.4 ± 0.1	0.2 ± 0.0	0.2 ± 0.0	0.9 ± 0.1	0.3 ± 0.0
cortex	0.7 ± 0.1	0.3 ± 0.0	0.3 ± 0.1	1.7 ± 0.0	0.4 ± 0.1
rest cerebrum	0.6 ± 0.1	0.3 ± 0.0	0.4 ± 0.1	1.2 ± 0.1	0.4 ± 0.0
cerebellum	0.6 ± 0.2	0.2 ± 0.0	0.3 ± 0.1	1.1 ± 0.1	0.3 ± 0.0
blood	0.6 ± 0.0	0.6 ± 0.1	0.5 ± 0.1	0.7 ± 0.0	0.5 ± 0.1

[a] Calculated as (radioactivity in counts per minute in striatum/weight of organ in grams)/(total counts recovered/body weight rat in grams). Data are expressed as mean ± SD; n = 3 per time point. [b] The 60 min time point biodistribution study was not performed with [^{18}F]**4**.

Table 5. Radioactivity Washout from Different Rat Brain Regions Calculated as 2 min-to-30 min Ratio[a] for [^{18}F]3, [^{18}F]4 and [^{18}F]1a

	striatum	hippocampus	cortex	cerebellum
[^{18}F]**3**	0.81	2.14	2.54	2.71
[^{18}F]**4**	1.80	3.08	4.24	3.82
[^{18}F]**1a**	0.95	1.95	2.77	3.27

[a] Calculated from the 2 and 30 min SUV values.

Biodistribution Studies with [^{18}F]3 and [^{18}F]4. [^{18}F]**3** and [^{18}F]**4** were evaluated in vivo in male Wistar rats by doing tissue distribution studies at 2, 30, and 60 min post injection (pi). Their brain pharmacokinetics was compared with the previously evaluated quinolinyl tracer [^{18}F]**1a**.[10] Table 3 shows the brain uptake upon dosing of the two pyridinyl derivatives [^{18}F]**3** and [^{18}F]**4** and of [^{18}F]**1a**. Both tracers produce a similar radioactivity uptake in brain (0.4% ID), which is lower than that of the quinolinyl derivative [^{18}F]**1a** (0.6% ID). Table 4 shows the SUVs (standardized uptake values) of the different studied brain regions and the blood upon dosing of [^{18}F]**3** and [^{18}F]**4**. Table 5 presents the relative retention in the studied brain regions for [^{18}F]**3**, [^{18}F]**4**, and [^{18}F]**1a**. For both tracers, at 2 min after tracer injection, the radioactivity concentration in the striatum was highest of all brain regions (SUV 1.0 for [^{18}F]**3**, SUV 2.3 for [^{18}F]**4** compared to SUV 1.6 for [^{18}F]**1a** at 2 min pi). Similar as with [^{18}F]**1a**, a significant washout of radioactivity from hippocampus, cortex, and cerebellum, brain regions which are devoid of PDE10A, was observed for [^{18}F]**3** and [^{18}F]**4** (Table 5; 2/30 min ratios >2.1). For [^{18}F]**3**, the tracer concentration in striatum increased as a function of time (2/30 min ratio = 0.81). This accumulation was as also observed with the previously studied [^{18}F]**1a** (2/30 min ratio = 0.95). For [^{18}F]**4**, washout from striatum was observed (2/30 min ratio = 1.80) but less significant as for the other brain regions. Retention (or slower washout) from striatum compared to other brain regions is consistent with the higher expression of PDE10A in this region. Because [^{18}F]**4** showed only limited striatum retention compared to [^{18}F]**3** and [^{18}F]**1a**, the 60 min biodistribution time point was not studied. For [^{18}F]**3** the highest radioactivity concentration in the striatum was 1.8 (SUV, at 60 min pi), which is lower than previously observed with the quinolinyl tracer [^{18}F]**1a** (SUV 2.6 at 60 min pi). Future small-animal PET imaging studies will reveal whether this striatum concentration is high enough to obtain significant signal-to-background PET images. Blood clearance of [^{18}F]**3** is relatively slow (SUV 0.6 at 2 and 30 min pi and SUV 0.5 at 60 min pi). This could be due to formation of radiometabolite(s). Future radiometabolite studies in plasma and perfused rat brain should clarify this.

Table 6. Radioactivity Striatum-to-Cerebellum Ratios at 2, 30, and 60 min Post Tracer Injection for [^{18}F]3, [^{18}F]4, and [^{18}F]1a

	striatum-to-cerebellum ratio[a]		
	2 min pi	30 min pi	60 min pi
[^{18}F]**3**	1.61	5.38	6.63
[^{18}F]**4**	2.07	4.38	
[^{18}F]**1a**	1.34	4.60	7.12

[a] Calculated from the SUV values of striatum and cerebellum.

There is large evidence that the cerebellum can be used as reference region in kinetic modeling. Therefore, apart from high striatum concentration, the nonspecific binding in the cerebellum should be low in order to obtain high striatum-to-cerebellum ratios and high quality images in vivo. Table 6 presents the striatum-to-cerebellum ratios for [^{18}F]**3**, [^{18}F]**4**, and [^{18}F]**1a** at 2, 30, and 60 min pi. Within analogy with [^{18}F]**1a**, there is an increase in the striatum-to-cerebellum ratio of [^{18}F]**3** from 2 min pi (1.61) to 30 min pi (5.38) to 60 min pi (6.63). Of the three studied tracers, [^{18}F]**3** has the highest striatum-to-cerebellum ratio at 30 min pi. At 60 min pi, the striatum-to-cerebellum ratio is lower for [^{18}F]**3** (6.63) compared to that of [^{18}F]**1a** (7.12). The increase of the striatum-to-cerebellum ratio from 30 to 60 min indicates that binding equilibrium was not yet reached at 60 min pi. This was also observed for [^{18}F]**1a**, and its slow kinetics was confirmed by baseline small-animal PET experiments. Future small-animal PET imaging experiments with [^{18}F]**3** are required to further study the kinetics of this tracer and to select which one has the best characteristics and should therefore be tested clinically for human brain imaging.

CONCLUSIONS

In summary, we have synthesized a series of analogues of the PDE10 inhibitor **1b** and its related radiotracer [^{18}F]**1a**, in which the 2-quinolinyl heterocycle has been replaced by differently substituted 2-pyridinyl moieties. From this investigation, we initially identified two potential PET ligand candidates, **3** and **4**, for in vivo imaging of the PDE10A enzyme. They were selected in

view of their good potency, selectivity, favorable lipophilicity, high level of brain penetration, and in vivo occupancy, and they were radiolabeled with [^{18}F]fluoride. Biodistribution studies in rats showed that the 3,5-dimethylpyridinyl derivative [^{18}F]**3** was the most promising PET ligand candidate, due to its good brain uptake, accumulation of radioactivity in the striatum, and higher striatum-to-cerebellum ratio. Small-animal PET imaging studies with [^{18}F]**3** are ongoing to further evaluate the kinetics of this tracer and its potential for human brain imaging, the results of which will be reported elsewhere.

EXPERIMENTAL SECTION

Chemistry. Materials and General Methods. All reagents and solvents were obtained commercially from Acros Organics, Aldrich, Fluka, Sigma, Merck, or Fischer Bioblock Scientific and used as supplied. Thin layer chromatography (TLC) was carried out on Silica Gel 60 F254 plates (Merck). Flash column chromatography was performed on silica gel, particle size 60 Å, mesh = 230−400 (Merck) under standard techniques. Automated flash column chromatography was performed using ready-to-connect cartridges on irregular silica gel, particle size 15−40 μm (Merck) on SPOT or LAFLASH system (Armen Instrument). Microwave assisted reactions were performed in a single-mode reactor: Biotage Initiator Sixty microwave reactor (Biotage) or in a multimode reactor: MicroSYNTH Labstation (Milestone, Inc.). Hydrogenation reactions were performed in a continuous flow hydrogenator H−CUBE from ThalesNano Nanotechnology Inc.

^{1}H NMR spectra were recorded either on a Bruker DPX-400 or on a Bruker AV-500 spectrometer (Bruker AG) with standard pulse sequences, operating at 400 and 500 MHz, respectively, using $CDCl_3$ and DMSO-d_6 as solvents. Chemical shifts (δ) are reported in parts per million (ppm) downfield from tetramethylsilane (δ = 0). Coupling constants are reported in hertz. Splitting patterns are defined by s (singlet), d (doublet), dd (double doublet), t (triplet), q (quartet), or m (multiplet). Liquid chromatography combined with mass spectrometry (LCMS) was performed on a HP 1100 HPLC system (Agilent Technologies) composed of a quaternary or binary pump with degasser, an autosampler, a column oven, a diode-array detector (DAD), and a column as specified in the respective methods below. Flow from the column was split to a MS spectrometer. The MS detector was configured either with an electrospray ionization source or an ESCI dual ionization source (electrospray combined with atmospheric pressure chemical ionization). ;Nitrogen was used as the nebulizer gas. Data acquisition was performed with MassLynx-Openlynx software or with Chemsation-Agilent Data Browser software. Melting points (mp) values are peak values and were obtained with experimental uncertainties that are commonly associated with this analytical method. For a number of compounds, noted as "DSC", melting points were determined with a DSC823e apparatus (Mettler-Toledo). Melting points were measured with a temperature gradient of 30 °C/min. Maximum temperature was 400 °C. For a number of compounds, melting points were determined in open capillary tubes on a Mettler FP62 apparatus. Melting points were measured with a temperature gradient of 10 °C/min. Maximum temperature was 300 °C. The melting point was read from a digital display.

Purities of all new nonradioactive compounds were determined by analytical reverse phase RP-HPLC using the area percentage method on the UV trace recorded at a wavelength of 254 nm and were found to have ≥95% purity unless otherwise specified. Final compounds that were isolated as succinic acid salts were also subjected to elemental analysis in order to determine their stoichiometry. More detailed information about the different analytical methods employed can be found in the Supporting Information.

*4-[3-(4-Benzyloxy-phenyl)-1-(2,2,2-trifluoroethyl)-1H-pyrazol-4-yl]-pyridine (**6a**).* A mixture of 4-[3-(4-benzyloxy-phenyl)-1*H*-pyrazol-4-yl]-pyridine (**5**)[17] (2.0 g, 6.11 mmol), 1,1,1-trifluoro-2-iodoethane (0.733 mL, 7.33 mmol), and Cs_2CO_3 (5.97 g, 18.3 mmol) in DMF (12 mL) was heated in a microwave oven at 120 °C for 20 min. After cooling to rt, the mixture was quenched with water and further extracted with EtOAc. The organic phase was dried over Na_2SO_4, filtered, and evaporated to dryness. The crude residue was purified by column chromatography (silicagel; MeCN/DIPE from 50/50 to 80/20). The desired fractions were collected and evaporated to dryness, yielding the desired intermediate compound **6a** as an oil (1.2 g, 38.4%). ^{1}H NMR (500 MHz, $CDCl_3$) δ 4.77 (q, J = 8.4 Hz, 2 H), 5.09 (s, 2 H), 6.93−7.00 (m, 2 H), 7.17−7.22 (m, 2 H), 7.33 (m, J = 7.2 Hz, 1 H), 7.36−7.42 (m, 4 H), 7.42−7.46 (m, 2 H), 7.71 (s, 1 H), 8.49−8.53 (m, 2 H). $C_{23}H_{18}F_3N_3O$. LCMS: Rt 4.86, m/z 410 [M + H]$^+$.

The corresponding regioisomer **7a** 4-[5-(4-benzyloxy-phenyl)-1-(2,2,2-trifluoroethyl)-1*H*-pyrazol-4-yl]-pyridine was also isolated from the chromatographic purification (0.4 g, 14.6%). ^{1}H NMR (400 MHz, $CDCl_3$) δ 4.57 (q, J = 8.1 Hz, 2 H), 5.14 (s, 2 H), 7.02−7.07 (m, 2 H), 7.11 (d, J = 9.0 Hz, 2 H), 7.23 (d, J = 8.7 Hz, 2 H), 7.35−7.40 (m, 1 H), 7.40−7.46 (m, 2 H), 7.46−7.51 (m, 2 H), 7.96 (s, 1 H), 8.42 (d, J = 6.1 Hz, 2 H). $C_{23}H_{18}F_3N_3O$. LCMS: Rt 4.87, m/z 410 [M + H]$^+$.

*4-[3-(4-Benzyloxy-phenyl)-1-(2-fluoroethyl)-1H-pyrazol-4-yl]-pyridine (**6b**).* A mixture of **5**[17] (6.7 g, 20.47 mmol), 1-bromo-2-fluoroethane (3.12 g, 24.56 mmol), and Cs_2CO_3 (20 g, 61.4 mmol) in DMF (42 mL) was heated in a MW oven at 150 °C for 5 min (the reaction was divided in 6 batches). After cooling to rt, the solid was discarded by filtration and the solution was quenched with water and further extracted with EtOAc. The organic phase was dried over Na_2SO_4, filtered, and evaporated to dryness. The crude residue was purified by column chromatography (silicagel; MeCN/DIPE from 30/70 to 80/20, and then again with EtOAc/heptane 70/30). The desired fractions were collected and evaporated to dryness, yielding the desired intermediate compound **6b** as an oil (4 g, 52.3%). ^{1}H NMR (400 MHz, $CDCl_3$) δ 4.46 (dt, J = 27.0, 4.9 Hz, 2 H), 4.83 (dt, J = 46.9, 4.6 Hz, 2 H), 5.08 (s, 2 H), 6.94−7.00 (m, 2 H), 7.16−7.21 (m, 2 H), 7.29−7.35 (m, 1 H), 7.35−7.42 (m, 4 H), 7.42−7.47 (m, 2 H), 7.69 (s, 1 H), 8.37−8.59 (m, 2 H). $C_{23}H_{20}FN_3O$. LCMS: Rt 4.22, m/z 374 [M + H]$^+$.

The corresponding regioisomer **7b** 4-[5-(4-benzyloxy-phenyl)-1-(2-fluoroethyl)-1*H*-pyrazol-4-yl]-pyridine was also isolated from the chromatographic purification (2 g, 26.2%). ^{1}H NMR (400 MHz, $CDCl_3$) δ 4.26 (dt, J = 24.7, 4.6 Hz, 2 H), 4.80 (dt, J = 46.9, 4.9 Hz, 2 H), 5.13 (s, 2 H), 7.06 (br s, 2 H), 7.07−7.14 (m, 2 H), 7.21−7.29 (m, 2 H), 7.33−7.39 (m, 1 H), 7.40−7.45 (m, 2 H), 7.45−7.51 (m, 2 H), 7.91 (s, 1 H), 8.42 (br s, 2 H). $C_{23}H_{20}FN_3O$. LCMS: Rt 4.26, m/z 374 [M + H]$^+$.

*4-[3-(4-Benzyloxy-phenyl)-1-(3-fluoro-propyl)-1H-pyrazol-4-yl]-pyridine (**6c**).* A mixture of **5**[17] (1 g, 3.05 mmol), DIAD (0.908 mL. 4.58 mmol), PPh_3 (1.2 g, 4.58 mmol), and 3-fluoro-1-propanol (0.357 g, 4.48 mmol) in THF (3 mL) was heated in a microwave oven at 120 °C for 20 min. The solvent was then evaporated until dryness, and the mixture was taken up in water and extracted with DCM. The organic phase was dried over Na_2SO_4, filtered, and evaporated to dryness. The crude residue was purified by column chromatography (silicagel; MeCN/DIPE from 50/50 to 100/0 and then with heptane/EtOAc from 50/50 to 30/70). The desired fractions were collected and evaporated to dryness, yielding the desired compound **6c** (0.4 g, 80% pure, 27%). ^{1}H NMR (400 MHz, CDCl3) δ 2.35 (dquin, J = 26.8, 6.0 Hz, 2 H), 4.34 (t, J = 6.7 Hz, 2 H), 4.51 (dt, J = 46.9, 5.8 Hz, 2 H), 5.09 (s, 2 H), 6.94−6.99 (m, 2 H), 7.15−7.21 (m, 2 H), 7.30−7.36 (m, 1 H), 7.36−7.42 (m, 4 H), 7.42−7.46 (m, 2 H), 7.64 (s, 1 H), 8.49 (d, J = 5.8 Hz, 2 H). $C_{24}H_{22}FN_3O$. LCMS: Rt 4.43, m/z 388 [M + H]$^+$.

The corresponding regioisomer **7c** 4-[5-(4-benzyloxy-phenyl)-1-(3-fluoro-propyl)-1*H*-pyrazol-4-yl]-pyridine was also isolated from the chromatographic purification (0.5 g, 50% pure). $C_{24}H_{22}FN_3O$. LCMS: Rt 3.22, m/z 388 [M + H]$^+$.

*4-[4-Pyridin-4-yl-1-(2,2,2-trifluoroethyl)-1H-pyrazol-3-yl]-phenol (**8a**).* Compound **6a** (1.1 g, 2.28 mmol) was dissolved in EtOH (50 mL) and

subjected to hydrogenation in a H-Cube system using 5% Pd/C as catalyst (full hydrogen mode, 1.5 mL/min) at 80 °C and atmospheric pressure. The solvent was evaporated to dryness in vacuo, affording intermediate compound **8a** as a white solid (0.55 g, 75.4%), which was used for the next reaction without further purification. $C_{16}H_{12}F_3N_3O$. LCMS: Rt 1.82, *m/z* 320 $[M + H]^+$.

*4-[1-(2-Fluoroethyl)-4-pyridin-4-yl-1H-pyrazol-3-yl]-phenol (**8b**).* Compound **6b** (4 g, 10.71 mmol) was dissolved in EtOH (200 mL) and subjected to hydrogenation in a H-Cube system using 5% Pd/C as catalyst (full hydrogen mode, 2.5 mL/min) at 80 °C and atmospheric pressure. The solvent was evaporated to dryness in vacuo, affording intermediate compound **8b** (2.5 g, 82.4%) that was used for the next reaction without further purification. ^{1}H NMR (400 MHz, DMSO-d_6) δ 4.48 (dt, J = 28.0, 4.7 Hz, 2 H), 4.84 (dt, J = 47.4, 4.7 Hz, 2 H), 6.72−6.83 (m, 2 H), 7.16−7.26 (m, 4 H), 8.22 (s, 1 H), 8.41−8.48 (m, 2 H), 9.60 (s, 1 H). $C_{16}H_{14}FN_3O$. LCMS: Rt 1.57, *m/z* 284 $[M + H]^+$.

*4-[1-(3-Fluoropropyl)-4-pyridin-4-yl-1H-pyrazol-3-yl]-phenol (**8c**).* Following the procedure for the preparation of compound **8b** but starting from intermediate **6c**, compound **8c** was synthesized (0.3 g, 80%). ^{1}H NMR (400 MHz, DMSO-d_6) δ 2.24 (dquin, J = 26.4, 6.5 Hz, 2 H), 4.26 (t, J = 7.2 Hz, 2 H), 4.53 (dt, J = 47.4, 5.5 Hz, 2 H), 6.73−6.80 (m, 2 H), 7.17−7.25 (m, 4 H), 8.21 (s, 1 H), 8.41−8.47 (m, 2 H), 9.59 (br s, 1 H). $C_{17}H_{16}FN_3O$. LCMS: Rt 1.81, *m/z* 298 $[M + H]^+$.

*General Procedure for the Synthesis of the Final Compounds **3**, **4**, **9**−**12**, **15**−**28**.* A mixture of compounds **8a** or **8b** or **8c** (1 equiv), the desired 2-hydroxymethylpyridine (1.5 equiv), DIAD (1.5 equiv), and PPh_3 (1.5 equiv) in THF (5 mL per mmol of starting material) was heated in a microwave oven at 120 °C for 20 min. After this time, the mixture was quenched with a saturated aqueous solution of Na_2CO_3 and extracted with DCM. The organic solvent was dried over Na_2SO_4 and evaporated to dryness. The crude residue was purified by chromatography. The desired fractions were collected and the solvent evaporated in vacuo to yield the desired final product.

*2-[[4-[1-(2-Fluoroethyl)-4-(4-pyridinyl)-1H-pyrazol-3-yl]phenoxy]-methyl]-3,5-dimethyl-pyridine·succinate (**3**).* Compound **3** was synthesized according to the general procedure starting from **8b** (0.2 g, 0.70 mmol) and 3,5-dimethyl-2-hydroxymethylpyridine. The final product was purified by chromatography (silicagel; EtOAc/MeOH from 100/0 to 95/5) to give compound **3** as a colorless oil. This oily compound was dissolved in MeOH (2 mL), and a solution of succinic acid (0.073 g, 0.619 mmol) in MeOH (2 mL) was slowly added. The solvent was evaporated to dryness, and the solid residue was washed several times with Et_2O, yielding the succinic acid salt of final compound **3** as a white solid (0.295 g, 80.3%); mp 138.8 °C (DSC). ^{1}H NMR (400 MHz, DMSO-d_6) δ 2.28 (s, 3 H), 2.35 (s, 3 H), 2.42 (s, 4 H), 4.49 (dt, J = 27.7, 4.7 Hz, 2 H), 4.85 (dt, J = 47.2, 4.6 Hz, 2 H), 5.16 (s, 2 H), 7.05 (d, J = 8.8 Hz, 2 H), 7.23 (d, J = 6.0 Hz, 2 H), 7.32 (d, J = 8.8 Hz, 2 H), 7.48 (s, 1 H), 8.23 (s, 2 H), 8.46 (d, J = 5.8 Hz, 2 H), 12.15 (br s, 2 H). $C_{24}H_{23}FN_4O \cdot C_4H_6O_4$. LCMS (ESI): Rt 3.08, *m/z* 403 $[M + H]^+$.

*2-[[4-[1-(2-Fluoroethyl)-4-(4-pyridinyl)-1H-pyrazol-3-yl]phenoxy]-methyl]-5-methoxy-pyridine (**4**).* Compound **4** was synthesized according to the general procedure, starting from **8b** (0.13 g, 0.34 mmol) and 5-methoxy-2-hydroxymethylpyridine.[25] The final product was purified by chromatography (silicagel; EtOAc/MeOH from 100/0 to 95/5) to give compound **4** as a white solid (0.12 g, 86.2%); mp 117.5 °C (DSC). ^{1}H NMR (400 MHz, $CDCl_3$) δ 3.87 (s, 3 H), 4.47 (dt, J = 27.0, 4.7 Hz, 2 H), 4.84 (dt, J = 46.9, 4.6 Hz, 2 H), 5.17 (s, 2 H), 6.97 (d, J = 8.8 Hz, 2 H), 7.18 (d, J = 6.0 Hz, 2 H), 7.22 (dd, J = 8.6, 3.0 Hz, 1 H), 7.39 (d, J = 8.8 Hz, 2 H), 7.44 (d, J = 8.6 Hz, 1 H), 7.70 (s, 1 H), 8.30 (d, J = 3.0 Hz, 1 H), 8.48 (d, J = 6.2 Hz, 2 H). $C_{23}H_{21}FN_4O_2$. LCMS (ESI): Rt 2.7, *m/z* 405 $[M + H]^+$, purity 94%.

*2-[[4-[1-(2-Fluoroethyl)-4-(4-pyridinyl)-1H-pyrazol-3-yl]phenoxy]-methyl]-6-methyl-pyridine·dihydrochloride (**9**).* Compound **9** was synthesized according to the general procedure, starting from **8b** (0.18 g, 0.51 mmol) and 6-methyl-2-hydroxymethylpyridine. The final product was purified by chromatography (silicagel; EtOAc/MeOH from 100/0 to 95/5) to give compound **9** as a colorless oil (0.05 g, 32%). Treatment of this oily compound with a solution of HCl (6 M in iPrOH) followed by crystallization from Et_2O/DCM afforded the dihydrochloric acid salt of compound **9** as a yellow solid; mp 227.2 °C (DSC). ^{1}H NMR (400 MHz, DMSO-d_6) δ 2.66 (s, 3 H), 4.56 (dt, J = 28.0, 4.6 Hz, 2 H), 4.88 (dt, J = 47.2, 4.6 Hz, 2 H), 5.37 (s, 2 H), 7.15 (d, J = 8.8 Hz, 2 H), 7.44 (d, J = 8.6 Hz, 2 H), 7.57 (d, J = 7.2 Hz, 1 H), 7.67 (d, J = 7.2 Hz, 1 H), 7.80 (d, J = 6.9 Hz, 2 H), 8.13 (t, J = 7.1 Hz, 1 H), 8.71 (s, 1 H), 8.74 (d, J = 6.9 Hz, 2 H). $C_{23}H_{21}FN_4O \cdot 2HCl$. LCMS (ESI): Rt 3.82, *m/z* 389 $[M + H]^+$.

*2-[[4-[1-(3-Fluoropropyl)-4-(4-pyridinyl)-1H-pyrazol-3-yl]phenoxy]-methyl]-6-methyl-pyridine·hydrochloride (**10**).* Compound **10** was obtained as described for derivative **9**, starting from **8c**. The final product was purified by chromatography (silicagel; MeCN/MeOH from 100/0 to 95/5) to give compound **10** as a colorless oil. Treatment of this oily compound with a solution of HCl (6 M in iPrOH) afforded the hydrochloric acid salt of compound **10** as white solid (0.075 g, 19.5%); mp 106.5 °C (DSC). ^{1}H NMR (500 MHz, DMSO-d_6) δ 2.20−2.34 (m, 2 H), 2.62 (s, 3 H), 4.33 (t, J = 6.9 Hz, 2 H), 4.54 (ddd, J = 47.3, 5.6, 5.5 Hz, 2 H), 5.32 (s, 2 H), 7.14 (d, J = 8.7 Hz, 2 H), 7.43 (d, J = 8.7 Hz, 2 H), 7.50 (d, J = 6.6 Hz, 1 H), 7.60 (d, J = 6.4 Hz, 1 H), 7.78 (d, J = 6.6 Hz, 2 H), 8.05 (br s, 1 H), 8.69 (s, 1 H), 8.73 (d, J = 6.4 Hz, 2 H). $C_{24}H_{23}FN_4O \cdot HCl$. LCMS: Rt 4.09, *m/z* 403 $[M + H]^+$, purity 90%.

*5-Methoxy-2-[[4-[4-(4-pyridinyl)-1-(**2**,**2**,2-trifluoroethyl)-1H-pyrazol-3-yl]phenoxy]methyl]-pyridine (**11**).* Compound **11** was synthesized according to the general procedure, starting from **8a** (0.15 g, 0.47 mmol) and 5-methoxy-2-hydroxymethylpyridine.[25] The final product was purified by chromatography (silicagel; EtOAc/MeOH from 100/0 to 95/5) to give compound **11** as a colorless oil that solidified on standing (0.11 g, 53.2%); mp 136.3 °C. ^{1}H NMR (400 MHz, $CDCl_3$) δ 3.87 (s, 3 H), 4.77 (q, J = 8.3 Hz, 2 H), 5.17 (s, 2 H), 6.97 (d, J = 9.0 Hz, 2 H), 7.19 (d, J = 6.2 Hz, 2 H), 7.23 (dd, J = 8.6, 3.0 Hz, 1 H), 7.38 (d, J = 8.8 Hz, 2 H), 7.44 (d, J = 8.6 Hz, 1 H), 7.71 (s, 1 H), 8.30 (d, J = 2.8 Hz, 1 H), 8.51 (d, J = 6.0 Hz, 2 H). $C_{23}H_{19}F_3N_4O_2$. LCMS (ESI): Rt 4.27, *m/z* 441 $[M + H]^+$.

*2-Bromo-6-[[4-[1-(2-fluoroethyl)-4-(4-pyridinyl)-1H-pyrazol-3-yl]-phenoxy]methyl]-pyridine·0.75succinate (**12**).* Compound **12** was synthesized according to the general procedure, starting from **8b** (0.30 g, 1.06 mmol) and 6-bromo-2-hydroxymethylpyridine. The final product was purified by chromatography (silicagel; EtOAc/heptane 70/30 and then Et_2O/DCM 70/30) to give compound **12** as a colorless oil (0.30 g, 53.1%). Compound **12** was converted into the corresponding succinic acid salt in a similar way as it is described above for final compound **3**, yielding derivative **12** as a white solid; mp 108.7 °C (DSC). ^{1}H NMR (400 MHz, DMSO-d_6) δ 2.42 (s, 3 H), 4.50 (dt, J = 27.7, 4.6 Hz, 2 H), 4.85 (dt, J = 47.2, 4.7 Hz, 2 H), 5.20 (s, 2 H), 7.06 (d, J = 8.8 Hz, 2 H), 7.22 (d, J = 6.0 Hz, 2 H), 7.35 (d, J = 8.8 Hz, 2 H), 7.59 (d, J = 7.4 Hz, 1 H), 7.63 (d, J = 7.9 Hz, 1 H), 7.82 (t, J = 7.7 Hz, 1 H), 8.24 (s, 1 H), 8.46 (d, J = 6.0 Hz, 2 H), 12.16 (br s, 1.5 H). $C_{22}H_{18}BrFN_4O \cdot 0.75C_4H_6O_4$. LCMS (ESI): Rt 3.22, *m/z* 453 $[M + H]^+$.

*2-[[4-[1-(2-Fluoroethyl)-4-(4-pyridinyl)-1H-pyrazol-3-yl]phenoxy]-methyl]-6-(trifluoromethyl)-pyridine (**13**).* Compound **12** (0.45 g, 0.725 mmol) was dissolved in DMF (3 mL), and then (fluorosulfonyl)-difluoroacetic acid methyl ester (0.46 mL, 3.62 mmol) and CuI (0.69 g, 3.62 mmol) were added to the solution. The reaction mixture was heated at 120 °C in a sealed tube for 2 h, and then it was allowed to reach rt and was quenched with an 1 M NaOH aq solution and finally was extracted with DCM. The organic solvent was dried over Na_2SO_4 and evaporated to dryness in vacuo. The residue was purified by column chromatography (silicagel; EtOAc/heptane 70/30 to 100/0). The desired fractions were collected, and the solvent was evaporated to dryness to give the desired compound as a yellow oil. The crude compound was further

purified by preparative HPLC (C18 XBridge 30 mm × 100 mm; aq NH_4HCO_3 pH 9/MeCN gradient from 80/20 to 0/100), affording compound **13** as a colorless oil. The compound was made solid after triturating with Et_2O/heptane, yielding final product **13** as a white foam (0.023 g, 7.2%). ^{1}H NMR (400 MHz, DMSO-d_6) δ 4.50 (dt, J = 27.8, 4.7 Hz, 2 H), 4.85 (dt, J = 47.2, 4.6 Hz, 2 H), 5.31 (s, 2 H), 7.09 (d, J = 8.8 Hz, 2 H), 7.22 (d, J = 6.0 Hz, 2 H), 7.35 (d, J = 8.8 Hz, 2 H), 7.89 (d, J = 7.9 Hz, 1 H), 7.89 (d, J = 7.6 Hz, 1 H), 8.18 (t, J = 7.9 Hz, 1 H), 8.24 (s, 1 H), 8.46 (d, J = 6.0 Hz, 2 H). $C_{23}H_{18}F_4N_4O$. LCMS (ESI): Rt 3.73, m/z 443 $[M + H]^+$, purity 91%.

*2-Cyclopropyl-6-[[4-[1-(2-fluoroethyl)-4-(4-pyridinyl)-1H-pyrazol-3-yl]phenoxy]methyl]-pyridine·succinate (**14**).* A mixture of compound **12** (0.14 g, 0.263 mmol), cyclopropyl-boronic acid (0.029 g, 0.341 mmol), and $Pd(PPh_3)_4$ (0.015 g, 0.013 mmol) in a mixture of aq Na_2CO_3/dioxane 1:1 (5 mL) was heated in a microwave oven at 130 °C for 15 min. After cooling to rt, the crude mixture was diluted with water and extracted with DCM. The organic solvent was dried over Na_2SO_4 and evaporated to dryness. The residue was purified by column chromatography (silicagel; EtOAc), the desired fractions were collected, and the solvent was evaporated to give the desired compound as an oil, which contained PPh_3O as a main impurity. This oil was further purified by preparative HPLC (C18 XBridge 19 mm × 100 mm; aq NH_4HCO_3 pH 9/MeCN gradient from 80/20 to 0/100), affording **14** as a colorless oil. The residue was dissolved in MeOH (2 mL), and a solution of succinic acid (0.017 g, 0.144 mmol) in MeOH (1 mL) was slowly added. The solvent was evaporated to dryness, and the residue was treated with DCM/DIPE, yielding the succinic acid salt of final compound **14** as a white solid (0.076 g, 54.4%); mp 91.3 °C (DSC). ^{1}H NMR (400 MHz, DMSO-d_6) δ 0.87−0.99 (m, 4 H), 2.05−2.16 (m, 1 H), 2.42 (s, 4 H), 4.49 (dt, J = 27.7, 4.6 Hz, 2 H), 4.85 (dt, J = 47.2, 4.7 Hz, 2 H), 5.10 (s, 2 H), 7.04 (d, J = 9.0 Hz, 2 H), 7.20−7.24 (m, 3 H), 7.26 (d, J = 7.4 Hz, 1 H), 7.33 (d, J = 8.8 Hz, 2 H), 7.68 (t, J = 7.7 Hz, 1 H), 8.24 (s, 1 H), 8.45 (d, J = 6.2 Hz, 2 H), 12.17 (br s, 1 H). $C_{25}H_{23}FN_4O \cdot C_4H_6O_4$. LCMS (ESI): Rt 4.19, m/z 415 $[M + H]^+$.

*3-Methoxy-2-[[4-[4-(4-pyridinyl)-1-(2,2,2-trifluoroethyl)-1H-pyrazol-3-yl]phenoxy]methyl]-pyridine (**15**).* Compound **15** was synthesized according to the general procedure starting from compound **8a** (0.15 g, 0.47 mmol) and (3-methoxypyridin-2-yl)methanol.[26] The crude mixture was purified by chromatography (silicagel; EtOAc/MeOH from 100/0 to 95/5) to give compound **15** as a white solid that was further crystallized from DIPE (0.12 g, 58%); mp 147 °C. ^{1}H NMR (400 MHz, $CDCl_3$) δ 3.89 (s, 3 H), 4.77 (q, J = 8.3 Hz, 2 H), 5.26 (s, 2 H), 7.02−7.07 (m, 2 H), 7.17−7.21 (m, 2 H), 7.23 (dd, J = 8.3, 1.6 Hz, 1 H), 7.27 (dd, J = 8.3, 4.6 Hz, 1 H), 7.34−7.41 (m, 2 H), 7.70 (s, 1 H), 8.25 (dd, J = 4.4, 1.6 Hz, 1 H), 8.49−8.53 (m, 2 H). $C_{23}H_{19}F_3N_4O_2$. LCMS (ESI): Rt 3.01, m/z 441 $[M + H]^+$.

*2-[[4-[1-(3-Fluoropropyl)-4-(4-pyridinyl)-1H-pyrazol-3-yl]phenoxy]methyl]-3-methoxy-pyridine (**16**).* Compound **16** was synthesized according to the general procedure starting from compound **8c** (0.16 g, 0.54 mmol) and (3-methoxypyridin-2-yl)methanol.[26] The crude mixture was purified by chromatography (silicagel; EtOAc/MeOH from 100/0 to 95/5) to give compound **16** as a white solid (0.09 g, 40%); mp 165.9 °C. ^{1}H NMR (500 MHz, $CDCl_3$) δ 2.34 (dquin, J = 26.9, 6.0, 6.0, 6.0, 6.0 Hz, 2 H), 3.89 (s, 3 H), 4.33 (t, J = 6.8 Hz, 2 H), 4.51 (dt, J = 47.1, 5.5 Hz, 2 H), 5.25 (s, 2 H), 7.01−7.06 (m, 2 H), 7.16−7.20 (m, 2 H), 7.23 (dd, J = 8.4, 1.2 Hz, 1 H), 7.27 (dd, J = 8.4, 4.7 Hz, 1 H), 7.34−7.41 (m, 2 H), 7.63 (s, 1 H), 8.25 (dd, J = 4.5, 1.6 Hz, 1 H), 8.45−8.50 (m, 2 H). $C_{24}H_{23}FN_4O_2$. LCMS (ESI): Rt 3.78, m/z 419 $[M + H]^+$.

*2-[[4-[1-(3-Fluoropropyl)-4-(4-pyridinyl)-1H-pyrazol-3-yl]phenoxymethyl]-5-methoxy-pyridine·0.5succinate (**17**).* Compound **17** was synthesized according to the general procedure starting from compound **8c** (0.25 g, 0.84 mmol) and 5-methoxy-2-hydroxymethylpyridine.[25] The crude mixture was purified by chromatography (silicagel; MeCN/MeOH from 100/0 to 95/5) to give compound **17** as a colorless oil that was converted into the corresponding succinic acid salt in a similar way as described above for final compound **3**, yielding the succinic acid salt of final compound **17** as a white solid (0.09 g, 25.6%); mp 126.6 °C (DSC). ^{1}H NMR (400 MHz, DMSO-d_6) δ 2.24 (dquin, J = 26.4, 6.2 Hz, 2 H), 2.41 (s, 2 H), 3.84 (s, 3 H), 4.27 (t, J = 6.9 Hz, 2 H), 4.52 (dt, J = 47.2, 5.7 Hz, 2 H), 5.11 (s, 2 H), 7.03 (br d, J = 8.8 Hz, 2 H), 7.17−7.25 (m, 2 H), 7.31 (br d, J = 8.8 Hz, 2 H), 7.43 (dd, J = 8.3, 3.0 Hz, 1 H), 7.50 (d, J = 8.6 Hz, 1 H), 8.23 (s, 1 H), 8.29 (d, J = 2.8 Hz, 1 H), 8.40−8.48 (m, 2 H), 12.18 (br s, 1 H). $C_{24}H_{23}FN_4O_2 \cdot 0.5C_4H_6O_4$. LCMS (ESI): Rt 3.97, m/z 419 $[M + H]^+$.

*2-[[4-[1-(2-Fluoroethyl)-4-(4-pyridinyl)-1H-pyrazol-3-yl]phenoxy]methyl]-3-methoxy-pyridine·succinate (**18**).* Compound **18** was synthesized according to the general procedure starting from compound **8b** (0.15 g, 0.52 mmol) and (3-methoxypyridin-2-yl)methanol.[26] The crude mixture was purified by chromatography (silicagel; EtOAc/MeOH from 100/0 to 95/5) to give compound **18** as a colorless oil, which was converted into the corresponding succinic acid salt in a similar way as described above for compound **3**, yielding the succinic acid salt of final compound **18** as a white solid (0.09 g, 32.5%); mp 178.9 °C (DSC). ^{1}H NMR (400 MHz, DMSO-d_6) δ 2.41 (s, 4 H), 3.86 (s, 3 H), 4.49 (dt, J = 27.7, 4.8 Hz, 2 H), 4.85 (dt, J = 47.2, 4.8 Hz, 2 H), 5.13 (s, 2 H), 7.03 (br d, J = 8.8 Hz, 2 H), 7.18−7.26 (m, 2 H), 7.31 (br d, J = 8.8 Hz, 2 H), 7.41 (dd, J = 8.3, 4.6 Hz, 1 H), 7.52 (dd, J = 8.4, 1.0 Hz, 1 H), 8.16 (dd, J = 4.6, 1.4 Hz, 1 H), 8.23 (s, 1 H), 8.43−8.48 (m, 2 H), 12.16 (br s, 2 H). $C_{23}H_{21}FN_4O_2 \cdot C_4H_6O_4$. LCMS (ESI): Rt 3.52, m/z 405 $[M + H]^+$.

*3-Fluoro-2-[[4-[1-(2-fluoroethyl)-4-(4-pyridinyl)-1H-pyrazol-3-yl]-phenoxy]methyl]-pyridine·1.2succinate (**19**).* Compound **19** was synthesized according to the general procedure starting from compound **8b** (0.10 g, 0.35 mmol) and (3-fluoropyridin-2-yl)methanol. The crude mixture was purified by chromatography (silicagel; EtOAc) to give compound **19** as a colorless oil that was converted into the corresponding succinic acid salt, in a similar way as described above for final compound **3**, yielding the succinic acid salt of final compound **19** as an amorphous solid (0.045 g, 24%). ^{1}H NMR (400 MHz, DMSO-d_6) δ 2.41 (s, 4.8 H), 4.50 (dt, J = 27.7, 4.6 Hz, 2 H), 4.85 (dt, J = 46.9, 4.9 Hz, 2 H), 5.25 (d, J = 2.1 Hz, 2 H), 7.04−7.10 (m, 2 H), 7.19−7.25 (m, 2 H), 7.30−7.37 (m, 2 H), 7.54 (dt, J = 8.5, 4.4 Hz, 1 H), 7.78−7.84 (m, 1 H), 8.24 (s, 1 H), 8.42−8.51 (m, 3 H), 12.26 (br s, 2.4 H). $C_{22}H_{18}F_2N_4O \cdot 1.2C_4H_6O_4$. LCMS (ESI): Rt 2.63, m/z 393 $[M + H]^+$.

*5-Bromo-2-[[4-[1-(2-fluoroethyl)-4-(4-pyridinyl)-1H-pyrazol-3-yl]-phenoxy]methyl]-pyridine (**20**).* Compound **20** was synthesized according to the general procedure starting from compound **8b** (0.10 g, 0.35 mmol) and (5-bromopyridin-2-yl)methanol. The crude mixture was purified by chromatography (silicagel; EtOAc/heptane 90:10) to give compound **20** that after treatment with Et_2O was obtained as a white solid (0.025 g, 15.6%); mp 125.8 °C. ^{1}H NMR (400 MHz, $CDCl_3$) δ 4.47 (dt, J = 27.0, 4.6 Hz, 2 H), 4.84 (dt, J = 46.9, 4.9 Hz, 2 H), 5.18 (s, 2 H), 6.93−6.98 (m, 2 H), 7.17−7.20 (m, 2 H), 7.38−7.42 (m, 2 H), 7.45 (dd, J = 8.3, 0.7 Hz, 1 H), 7.70 (d, J = 0.5 Hz, 1 H), 7.85 (dd, J = 8.3, 2.3 Hz, 1 H), 8.47−8.51 (m, 2 H), 8.66 (dd, J = 2.3, 0.5 Hz, 1 H). $C_{22}H_{18}BrFN_4O$. LCMS (ESI): Rt 3.29, m/z 453 $[M + H]^+$.

*6-[[4-[1-(2-Fluoroethyl)-4-(4-pyridinyl)-1H-pyrazol-3-yl]phenoxy]methyl]-3-pyridinecarbonitrile (**21**).* Compound **21** was synthesized according to the general procedure starting from compound **8b** (0.18 g, 0.63 mmol) and 6-(hydroxymethyl)nicotinonitrile. The crude mixture was purified by chromatography (silicagel; EtOAc) to give compound **21** as white solid (0.1 g, 39.4%); mp >300 °C (dec). ^{1}H NMR (500 MHz, $CDCl_3$) δ 4.48 (dt, J = 27.2, 4.6 Hz, 2 H), 4.85 (dt, J = 46.8, 4.6 Hz, 2 H), 5.28 (s, 2 H), 6.96 (br d, J = 9.0 Hz, 2 H), 7.16−7.21 (m, 2 H), 7.39−7.45 (m, 2 H), 7.72 (d, J = 8.4 Hz, 1 H), 7.71 (s, 1 H), 8.00 (dd, J = 8.1, 2.0 Hz, 1 H), 8.49 (br d, J = 6.1 Hz, 2 H), 8.87 (d, J = 1.4 Hz, 1 H). $C_{23}H_{18}FN_5O$. LCMS (ESI): Rt 3.11, m/z 400 $[M + H]^+$.

*2-[[4-[1-(2-Fluoroethyl)-4-(4-pyridinyl)-1H-pyrazol-3-yl]phenoxy]-methyl]-5-(trifluoromethyl)-pyridine (**22**).* Compound **22** was synthesized according to the general procedure starting from compound **8b** (0.055 g, 0.19 mmol) and (5-trifluoromethyl-pyridin-2-yl)methanol. The crude mixture was purified by chromatography (silicagel; EtOAc/heptane 70:30) and then by HPLC (C18 XBridge 30 mm × 100 mm; aq NH_4HCO_3, pH 9/MeCN gradient from 80/20 to 0/100) to give compound **22** as a white solid (0.025 g, 29.4%); mp 133.2 °C (DSC). ^{1}H NMR (400 MHz, $CDCl_3$) δ 4.48 (dt, J = 27.0, 4.6 Hz, 2 H), 4.84 (dt, J = 46.9, 4.6 Hz, 2 H), 5.29 (s, 2 H), 6.95−7.00 (m, 2 H), 7.16−7.21 (m, 2 H), 7.39−7.45 (m, 2 H), 7.70 (d, J = 6.5 Hz, 1 H), 7.70 (s, 1 H), 7.97 (dd, J = 8.2, 2.0 Hz, 1 H), 8.46−8.53 (m, 2 H), 8.86 (br s, 1 H). $C_{23}H_{18}F_4N_4O$. LCMS (ESI): Rt 3.37, m/z 443 $[M + H]^+$.

*5-Cyclopropyl-2-[[4-[1-(2-fluoroethyl)-4-(4-pyridinyl)-1H-pyrazol-3-yl]phenoxy]methyl]-pyridine (**23**).* Compound **23** was synthesized according to the general procedure starting from compound **8b** (0.15 g, 0.53 mmol) and (5-cyclopropyl-pyridin-2-yl)methanol, which was prepared following a similar experimental procedure to that described for compound **14**. The crude mixture was purified by chromatography (silicagel; EtOAc/heptane from 80:20 to 100:0) to give compound **23** as a colorless oil that solidified on standing (0.1 g, 45.6%); mp >300 °C (dec.). ^{1}H NMR (500 MHz, $CDCl_3$) δ 0.67−0.78 (m, 2 H), 0.96−1.10 (m, 2 H), 1.87−1.95 (m, 1 H), 4.47 (dt, J = 26.9, 4.8 Hz, 2 H), 4.84 (dt, J = 47.1, 4.7 Hz, 2 H), 5.19 (s, 2 H), 6.94−6.99 (m, 2 H), 7.16−7.21 (m, 2 H), 7.32 (dd, J = 8.1, 2.3 Hz, 1 H), 7.36−7.41 (m, 3 H), 7.70 (s, 1 H), 8.40 (d, J = 2.0 Hz, 1 H), 8.48 (br d, J = 6.1 Hz, 2 H). $C_{25}H_{23}FN_4O$. LCMS (ESI): Rt 3.24, m/z 415 $[M + H]^+$.

*2-[[4-[1-(2-Fluoroethyl)-4-(4-pyridinyl)-1H-pyrazol-3-yl]phenoxy]-methyl]-6-methoxy-pyridine·succinate (**24**).* Compound **24** was synthesized according to the general procedure starting from compound **8b** (0.2 g, 0.7 mmol) and (6-methoxy-pyridin-2-yl)methanol. The crude mixture was purified by chromatography (silicagel; EtOAc) and then by HPLC (C18 XBridge 30 mm × 100 mm; aq NH_4HCO_3, pH 9/MeCN gradient from 80/20 to 0/100) to give compound **24** as a colorless oil (0.075 g, 26.4%). This material was converted into the corresponding succinic acid salt, in a similar way as it is described above for **3**, yielding the succinic acid salt of final compound **24** as a white solid; mp 113.2 °C (DSC). ^{1}H NMR (500 MHz, DMSO-d_6) δ 2.42 (s, 4 H), 3.86 (s, 3 H), 4.49 (dt, J = 27.7, 4.9 Hz, 2 H), 4.85 (dt, J = 47.4, 4.9 Hz, 2 H), 5.11 (s, 2 H), 6.77 (d, J = 8.4 Hz, 1 H), 7.03−7.09 (m, 2 H), 7.12 (d, J = 7.2 Hz, 1 H), 7.20−7.25 (m, 2 H), 7.31−7.36 (m, 2 H), 7.74 (dd, J = 8.2, 7.4 Hz, 1 H), 8.24 (s, 1 H), 8.42−8.49 (m, 2 H), 12.17 (br s, 2 H). $C_{23}H_{21}FN_4O_2 \cdot C_4H_6O_4$. LCMS (ESI): Rt 4.16, m/z 405 $[M + H]^+$.

*2-Ethoxy-6-[[4-[1-(2-fluoroethyl)-4-(4-pyridinyl)-1H-pyrazol-3-yl]-phenoxy]methyl]-pyridine·succinate (**25**).* Compound **25** was synthesized according to the general procedure starting from compound **8b** (0.12 g, 0.42 mmol) and (6-ethoxypyridin-2-yl)methanol. The crude mixture was purified by chromatography (silicagel; EtOAc) and then by HPLC (C18 XBridge 30 mm × 100 mm; aq NH_4HCO_3, pH 9/MeCN gradient from 80/20 to 0/100) to give compound **25** as a colorless oil (0.080 g, 45.4%). This material was converted into the corresponding succinic acid salt in a similar way as described above for **3**, yielding the succinic acid salt of final compound **25** as a white solid; mp 119.6 °C (DSC). ^{1}H NMR (400 MHz, DMSO-d_6) δ 1.31 (t, J = 6.9 Hz, 3 H), 2.41 (s, 4 H), 4.30 (q, J = 7.2 Hz, 2 H), 4.49 (dt, J = 27.7, 4.6 Hz, 2 H), 4.85 (dt, J = 47.4, 4.9 Hz, 2 H), 5.10 (s, 2 H), 6.74 (d, J = 8.3 Hz, 1 H), 7.03−7.08 (m, 2 H), 7.10 (d, J = 7.2 Hz, 1 H), 7.20−7.25 (m, 2 H), 7.29−7.37 (m, 2 H), 7.73 (dd, J = 8.2, 7.3 Hz, 1 H), 8.24 (s, 1 H), 8.43−8.48 (m, 2 H), 12.19 (br s, 2 H). $C_{24}H_{23}FN_4O_2 \cdot C_4H_6O_4$. LCMS (ESI): Rt 3.56, m/z 419 $[M + H]^+$.

*6-[[4-[1-(2-Fluoroethyl)-4-(4-pyridinyl)-1H-pyrazol-3-yl]phenoxy]-methyl]-2-pyridinecarbonitrile (**26**).* Compound **26** was synthesized according to the general procedure starting from compound **8b** (0.2 g, 0.70 mmol) and 6-hydroxymethyl-2-cyanopyridine.[27] The crude mixture was purified by chromatography (silicagel; EtOAc/MeOH from 100:0 to 95:5) to give compound **26** that after treatment with Et_2O was isolated as a white solid (0.115 g, 40.8%); mp 148.7 °C. ^{1}H NMR (400 MHz, DMSO-d_6) δ 4.50 (dt, J = 27.5, 4.4 Hz, 2 H), 4.85 (dt, J = 47.4, 4.9 Hz, 2 H), 5.28 (s, 2 H), 7.05−7.10 (m, 2 H), 7.23 (br d, J = 4.4 Hz, 2 H), 7.33−7.38 (m, 2 H), 7.89 (dd, J = 7.9, 0.9 Hz, 1 H), 8.03 (dd, J = 7.6, 0.9 Hz, 1 H), 8.13 (t, J = 7.7 Hz, 1 H), 8.24 (s, 1 H), 8.47 (br s, 2 H). $C_{23}H_{18}FN_5O$. LCMS (ESI): Rt 2.68, m/z 400 $[M + H]^+$.

*3-Bromo-2-[[4-[1-(2-fluoroethyl)-4-(4-pyridinyl)-1H-pyrazol-3-yl]-phenoxy]methyl]-6-methoxy-pyridine (**27**).* Compound **27** was synthesized according to the general procedure starting from compound **8b** (0.13 g, 0.46 mmol) and 3-bromo-2-(hydroxymethyl)-6-methoxypyridine. The crude mixture was purified by chromatography (silicagel; EtOAc/heptane 70:30) and then by HPLC (C18 XBridge 30 mm × 100 mm, aq NH_4HCO_3, pH 9/MeCN gradient from 80/20 to 0/100) to yield compound **27** as white solid (0.12 g, 54%); mp 119.2 °C. ^{1}H NMR (400 MHz, $CDCl_3$) δ 3.85 (s, 3 H), 4.47 (dt, J = 26.8, 4.6 Hz, 2 H), 4.84 (dt, J = 46.9, 4.6 Hz, 2 H), 5.22 (s, 2 H), 6.61 (d, J = 8.6 Hz, 1 H), 6.98−7.03 (m, 2 H), 7.17−7.21 (m, 2 H), 7.36−7.41 (m, 2 H), 7.68−7.72 (m, 2 H), 8.46−8.51 (m, 2 H). $C_{23}H_{20}BrFN_4O_2$. LCMS (ESI): Rt 4.58, m/z 483 $[M + H]^+$.

*2-[[4-[1-(2-Fluoroethyl)-4-(4-pyridinyl)-1H-pyrazol-3-yl]phenoxy-methyl]-3,4,5-trimethyl-pyridine·succinate (**28**).* Compound **28** was synthesized according to the general procedure starting from compound **8b** (0.14 g, 0.5 mmol) and (3,4,5-trimethylpyridin-2yl)methanol.[28] The crude mixture was purified by chromatography (silicagel; EtOAc/MeOH from 100/0 to 95/5) to give compound **28** as a colorless oil. This derivative was converted into the corresponding succinic acid salt in a similar way as described above for compound **3**, affording the succinic acid salt of final compound **28** as a white solid (0.15 g, 56.8%); mp 197.1 °C (DSC). ^{1}H NMR (500 MHz, DMSO-d_6) δ 2.26 (s, 3 H), 2.30 (s, 3 H), 2.35 (s, 3 H), 2.48 (s, 4 H), 4.55 (dt, J = 27.7, 4.6 Hz, 2 H), 4.91 (dt, J = 47.1, 4.6 Hz, 2 H), 5.23 (s, 2 H), 7.09−7.14 (m, 2 H), 7.27−7.31 (m, 2 H), 7.35−7.41 (m, 2 H), 8.21 (s, 1 H), 8.28 (s, 1 H), 8.50−8.54 (m, 2 H), 12.22 (br s, 2 H). $C_{25}H_{25}FN_4O \cdot C_4H_6O_4$. LCMS (ESI): Rt 3.53, m/z 417 $[M + H]^+$.

*4-(3,5-Dimethyl-pyridin-2-ylmethoxy)-benzoic Acid Methyl Ester (**30**).* Di-*tert*-butylazadicarboxylate (6.55 g, 28.43 mmol) was added portionwise to a stirred solution of 3,5-dimethyl-2-hydroxypyridine (3 g, 21.87 mmol), methyl-4-hydroxybenzoate (**29**, 3.66 g, 24.05 mmol), and PPh_3 (7.45 g, 28.43 mmol) in THF (30 mL). The reaction mixture was heated under microwave irradiation at 120 °C for 20 min (reaction divided in two batches). Then the mixture was diluted with water, extracted with DCM, dried over Na_2SO_4, and concentrated until dryness. The crude residue was purified by chromatography (silicagel, heptane/EtOAc from 80/20 to 50/50), and the desired fractions were collected and evaporated to dryness affording compound **30** as a yellow oil around ∼60% pure (84.5% yield) that was used for next reaction without further purification. ^{1}H NMR (500 MHz, $CDCl_3$) δ 2.31 (s, 3 H), 2.38 (s, 3 H), 3.85 − 3.90 (m, 3 H), 5.23 (s, 2 H), 7.01−7.07 (m, 2 H), 7.33 (s, 1 H), 7.93−8.01 (m, 2 H), 8.27 (s, 1 H). $C_{16}H_{17}NO_3$. LCMS: Rt 2.53 m/z 272 $[M + H]^+$.

*4-(3,5-Dimethyl-pyridin-2-ylmethoxy)-N-methoxy-N-methyl-benzamide (**31**).* An aqueous 2 M NaOH solution (18.5 mL) was added to **30** (18.45 mmol) dissolved in a mixture THF/MeOH (1:2 30 mL), and the reaction mixture was stirred at rt for 6 h. After this time, the organic solvent was evaporated and the aqueous phase washed with EtOAc and then acidified (HCl, 1 M in H_2O) until pH = 5−6. The white solid obtained was filtered off, dried, and then redissolved in $SOCl_2$ (20 mL) and stirred at rt for 6 h. The mixture was then concentrated until dryness, the crude residue was redissolved in THF (60 mL), and then Et_3N (7.4 mL, 53.3 mmol) and *N*,*O*-dimethylhydroxylamine hydrochloride (3.9 g, 40 mmol) were added cautiosly. This reaction mixture was stirred at rt for 2 h. Then, more Et_3N (7.4 mL, 53.3 mmol) was added and the mixture was stirred additionally for 1 h. After this time, water was added,

and after extraction with EtOAc, the organic layer was separated, dried over Na_2SO_4, filtered, and evaporated to dryness. The crude product was purified by chromatography (silicagel, heptane/EtOAc from 40/60 to 0/100), and the desired fractions were collected and the solvent evaporated in vacuo to give compound **31** as an orange oil (3 g, 54%). ^{1}H NMR (500 MHz, $CDCl_3$) δ 2.31 (s, 3 H), 2.39 (s, 3 H), 3.35 (s, 3 H), 3.56 (s, 3 H), 5.21 (s, 2 H), 7.02 (d, J = 8.7 Hz, 2 H), 7.34 (s, 1 H), 7.70 (d, J = 8.7 Hz, 2 H), 8.27 (s, 1 H). $C_{17}H_{20}N_2O_3$. LCMS: Rt 2.59 m/z 301 $[M + H]^+$.

*1-[4-(3,5-Dimethyl-pyridin-2-ylmethoxy)-phenyl]-2-pyridin-4-yl-ethanone (**32**).* To a solution of LDA (2 M in THF, 25 mL) in THF (22 mL) stirred at 0 °C, 4-picoline (4.8 mL, 50 mmol) was added dropwise. After 30 min, this solution was cooled down to −78 °C and 15 mL of this solution was added dropwise to a mixture of **31** (3 g, 10 mmol) dissolved in THF (38 mL) at −78 °C. The reaction mixture was stirred at this temperature for 30 min. Then it was quenched with water, concentrated, and extracted with DCM. The organic layer was separated, dried over Na_2SO_4, filtered, and evaporated to dryness The crude compound obtained was triturated with Et_2O, affording compound **32** (2.35 g, 71%) as a pale-yellow solid that was used as such in the next reaction step. ^{1}H NMR (400 MHz, $CDCl_3$) δ 2.32 (s, 3 H), 2.39 (s, 3 H), 4.22 (s, 2 H), 5.26 (s, 2 H), 7.07−7.12 (m, 2 H), 7.18−7.22 (m, 2 H), 7.35 (br s, 1 H), 7.93−7.99 (m, 2 H), 8.28 (d, J = 0.9 Hz, 1 H), 8.53−8.58 (m, 2 H). $C_{21}H_{20}N_2O_2$. LCMS: Rt 3.32 m/z 333 $[M + H]^+$.

*3,5-Dimethyl-2-[4-(4-pyridin-4-yl-2H-pyrazol-3-yl)-phenoxymethyl]-pyridine (**33**).* A solution of compound **32** (2.35 g, 7.07 mmol) in DMF−dimethylacetal (15 mL) was stirred under reflux for 1 h. After evaporation of the solvent, the crude mixture was redissolved in MeOH (25 mL) and $NH_2NH_2 \cdot H_2O$ (60% in H_2O, 10.6 mmol) was added. The mixture was heated under reflux for 1 h, and then the solvent was evaporated in vacuo and the crude mixture was purified by chromatography (silica, DCM/MeOH from 100/0 to 90/10). The desired fractions were collected and evaporated to dryness, yielding the desired compound **33** as an off-white solid (0.9 g, 35.7%). ^{1}H NMR (400 MHz, $CDCl_3$) δ 2.33 (s, 3 H), 2.41 (s, 3 H), 5.16 (s, 2 H), 6.98−7.04 (m, 2 H), 7.20−7.25 (m, 2 H), 7.31−7.36 (m, 2 H), 7.36 (br s, 1 H), 7.80 (s, 1 H), 8.31 (d, J = 0.9 Hz, 1 H), 8.46−8.52 (m, 2 H), 11.66 (br s, 1 H). $C_{22}H_{20}N_4O$. LCMS: Rt 3.63 m/z 357 $[M + H]^+$.

*2-[3-[4-(3,5-Dimethyl-pyridin-2-ylmethoxy)-phenyl]-4-pyridin-4-yl-pyrazol-1-yl]-ethanol (**35a**).* A mixture of compound **33** (0.25 g, 0.7 mmol), methyl bromoacetate (0.08 mL, 0.84 mmol), and Cs_2CO_3 (0.685 g, 2.1 mmol) in DMF (8 mL) was stirred at rt for 3 h. Then the reaction mixture was quenched with water and extracted with EtOAc, and the organic phase was separated, dried over Na_2SO_4, and the solvent evaporated in vacuo. The crude residue was then redissolved in MeOH/DCM (1:4, 5 mL), $NaBH_4$ (0.1 g, 2.68 mmol) was added, and the reaction mixture was stirred at rt for 1 h. Then it was quenched with water and extracted with DCM. The organic layer was separated, dried over Na_2SO_4, filtered, and evaporated to dryness. The crude residue was purified by chromatography (silicagel, EtOAC/MeOH from 100/0 to 90/10), the desired fractions were collected and evaporated in vacuo to give compound **35a** as a white solid (0.06 g, 28%). ^{1}H NMR (500 MHz, $CDCl_3$) δ 2.32 (s, 3 H), 2.41 (s, 3 H), 3.22 (br s, 1 H), 4.09 (t, J = 4.9 Hz, 2 H), 4.31 (t, J = 4.9 Hz, 2 H), 5.20 (s, 2 H), 7.01 (d, J = 8.7 Hz, 2 H), 7.18 (d, J = 6.1 Hz, 2 H), 7.34 (s, 1 H), 7.38 (d, J = 8.7 Hz, 2 H), 7.66 (s, 1 H), 8.27 (s, 1 H), 8.49 (d, J = 5.8 Hz, 2 H). $C_{24}H_{24}N_4O_2$. LCMS: Rt 2.60 m/z 401 $[M + H]^+$.

The corresponding regioisomer **35b** 2-[5-[4-(3,5-dimethyl-pyridin-2-ylmethoxy)-phenyl]-4-pyridin-4-yl-pyrazol-1-yl]-ethanol was also isolated from the chromatographic purification (0.02 g, 10%). ^{1}H NMR (400 MHz, $CDCl_3$) δ 2.32 (s, 3 H), 2.41 (s, 3 H), 2.56 (br s, 1 H), 4.06−4.12 (m, 2 H), 4.27−4.36 (m, 2 H), 5.21 (s, 2 H), 7.02−7.07 (m, 2 H), 7.29−7.34 (m, 4 H), 7.35 (br s, 1 H), 7.79 (s, 1 H), 8.27 (br s, 1 H), 8.38 (d, J = 6.5 Hz, 2 H). $C_{24}H_{24}N_4O_2$. LCMS: Rt 2.55 m/z 401 $[M + H]^+$.

*6-[4-[1-(2-Fluoroethyl)-4-pyridin-4-yl-1H-pyrazol-3-yl]-phenoxymethyl]-pyridin-3-ol (**37**).* To a solution of compound **8b** (0.15 g, 0.53 mmol), 5-(methoxy-ethoxymethoxy)-2-hydroxymethylpyridine (**36**)[20] (0.17 g, 0.8 mmol), and PPh_3 (0.182 g, 0.8 mmol) in THF (5 mL), di-*tert*-butylazadicarboxylate (0.208 g, 0.8 mmol) was added portionwise. The reaction mixture was heated in a microwave oven at 120 °C for 30 min. The mixture was diluted with an aq satd solution of Na_2CO_3 and extracted with EtOAc, and the organic layer was separated, dried over Na_2SO_4, filtered, and concentrated in vacuo. The residue was purified by chromatography (silicagel, EtOAc/MeOH from 100/0 to 95/5) to give the desired compound as a colorless oil (purity ∼70%). This oily product was then dissolved in DCM (6 mL), and TFA (3 mL) was added at 0 °C. Then the mixture was allowed to reach rt and was further stirred for 24 h. The solvent was evaporated, and the crude compound was taken up in a saturated aq $NaHCO_3$ solution and extracted several times with DCM. The organic layers were combined and dried over Na_2SO_4, filtered, and the solvent was evaporated to dryness. The solid residue was thoroughly washed with Et_2O, yielding finally compound **37** as a white solid (0.115 g, 70.5%). ^{1}H NMR (400 MHz, DMSO-d_6) δ 4.51 (dt, J = 28.0, 4.6 Hz, 2 H), 4.85 (dt, J = 47.4, 4.9 Hz, 2 H), 5.07 (s, 2 H), 7.05 (d, J = 8.8 Hz, 2 H), 7.21 (dd, J = 8.4, 2.9 Hz, 1 H), 7.35 (d, J = 8.8 Hz, 2 H), 7.39 (d, J = 8.3 Hz, 1 H), 7.41−7.47 (m, 2 H), 8.13 (d, J = 2.8 Hz, 1 H), 8.39 (br s, 1 H), 8.51−8.59 (m, 2 H), 10.04 (br s, 1 H). $C_{22}H_{19}FN_4O_2$. LCMS: Rt 1.56 m/z 391 $[M + H]^+$.

*[4-Pyridin-4-yl-3-[4-(quinolin-2-ylmethoxy)-phenyl]-pyrazol-1-yl]-acetic Acid Methyl Ester (**39a**) and [4-Pyridin-4-yl-5-[4-(quinolin-2-ylmethoxy)-phenyl]-pyrazol-1-yl]-acetic Acid Methyl Ester (**39b**).* To a stirred solution of **38**[11] (0.5 g, 1.33 mmol) in DMF (10 mL), methyl bromoacetate (0.15 mL, 1.6 mmol) and Cs_2CO_3 (1.3 g, 3.99 mmol) were added. The mixture was stirred at rt for 3 h, and then it was quenched with water and extracted with EtOAc. The organic layer was separated, dried over Na_2SO_4, filtered, and evaporated to dryness. The crude residue was purified by chromatography (silicagel; EtOAc/MeOH from 100/0 to 95/5). The desired fractions were collected and evaporated in vacuo to yield a mixture of the two regioisomers **39a** and **39b** that were used in the next reaction step without further purification (0.47 g, 47%). $C_{27}H_{22}N_4O_3$. LCMS: Rt 2.91 (same retention time for both isomers) m/z 451 $[M + H]^+$.

*2-[3-[4-(5-Methoxy-pyridin-2-ylmethoxy)-phenyl]-4-pyridin-4-yl-pyrazol-1-yl]-ethanol (**40a**).* Step 1: The mixture of intermediate compounds **39a** and **39b** (0.37 g, 0.82 mmol) was dissolved in EtOH (20 mL) and subjected to hydrogenation in a H-Cube system using 5% Pd/C as catalyst (full hydrogen mode, 1.5 mL/min) at 70 °C and atmospheric pressure. The solvent was evaporated to dryness to give yellow oil that was solidified by treatment with DCM, yielding a mixture of the two hydroxyphenyl isomers that was used for the next reaction without further purification (0.170 g, 67%). $C_{17}H_{15}N_3O_3$. LCMS: Rt 0.95 (major regioisomer), Rt 1.00 (minor regioisomer), m/z 310 $[M + H]^+$. Step 2: To this mixture of the two regioisomers (0.17 g, 0.550 mmol) in THF (4 mL) was added (5-methoxypyridin-2-yl)methanol (0.115 g, 0.825 mmol), DIAD (0.190 g, 0.825 mmol), and PPh_3 (0.216 g, 0.825 mmol). The reaction mixture was heated in a microwave oven at 120 °C for 20 min. After this time, the solvent was evaporated to dryness and the crude residue was purified by column chromatography (silicagel; EtOAc/MeOH 100/0 to 95/5). The desired fractions were collected, and the solvent was evaporated to yield a mixture of the corresponding two regioisomers that was used for the next reaction without further purification. Step 3: To a stirred solution of the previous mixture of isomers (0.18 g, 0.418 mmol) in DCM/MeOH (4:1, 5 mL) was added $NaBH_4$ (0.079 g, 2.09 mmol), and the reaction mixture was stirred at rt for 3 h. The mixture was then quenched with water, extracted with more DCM, and the organic layer was separated and dried over Na_2SO_4, filtered, and evaporated to dryness. The crude residue was purified by column chromatography (silicagel; EtOAc/MeOH from 100/0 to 90/10).

The desired fractions were collected and evaporated in vacuo to yield compound **40a** as a foam (0.09 g, 53.5%). The other regioisomer **40b** was not isolated from the chromatographic separation. ^{1}H NMR (500 MHz, CDCl3) δ 3.20 (br s, 1 H), 3.88 (s, 3 H), 4.10 (br t, J = 4.0 Hz, 2 H), 4.31 (t, J = 4.6 Hz, 2 H), 5.17 (s, 2 H), 6.94−7.01 (m, 2 H), 7.15−7.20 (m, 2 H), 7.24 (dd, J = 8.7, 2.9 Hz, 1 H), 7.36−7.41 (m, 2 H), 7.45 (d, J = 8.4 Hz, 1 H), 7.67 (s, 1 H), 8.30 (d, J = 2.9 Hz, 1 H), 8.44−8.52 (m, 2 H). $C_{23}H_{22}N_4O_3$. LCMS: Rt 2.87, m/z 403 $[M + H]^+$.

Radiochemistry. All reagents and solvents were obtained commercially from Acros Organics, Aldrich, Fluka, Sigma or Merck and used as supplied. HPLC analysis was performed on a LaChrom Elite HPLC system (Hitachi, Darmstadt, Germany) connected to a UV spectrometer set at 254 nm. The HPLC eluate after passage through the UV detector was led over a 3 in. NaI(Tl) scintillation detector connected to a single channel analyzer (Gabi box, Raytest, Straubenhardt Germany).

*2-[[4-[1-(2-[^{18}F]Fluoroethyl)-4-(4-pyridinyl)-1H-pyrazol-3-yl]phenoxy]methyl]-3,5-dimethyl-pyridine ([^{18}F]**3**) Method A Starting from Precursor Compound **33** and [^{18}F]Fluoroethyl Bromide.* [^{18}F]fluoride ([^{18}F]F$^-$) was produced by an [^{18}O(p,n)^{18}F] reaction by irradiation of 2 mL of 97% enriched [^{18}O]H_2O (Rotem HYOX18, Rotem Industries, Beer Sheva, Israel) in a niobium target using 18 MeV protons from a Cyclone 18/9 cyclotron (Ion Beam Applications, Louvain-la-Neuve, Belgium). After irradiation, the resultant [^{18}F]F$^-$ was separated from [^{18}O]H_2O using a SepPak Light Accell plus QMA anion exchange cartridge (Waters, CO_3^{2-} form). [^{18}F]F$^-$ was eluted from the cartridge using a 0.75 mL of a solution containing K_2CO_3 (2.47 mg) and Kryptofix 222 (27.92 mg) dissolved in H_2O/MeCN (0.75 mL; 5:95 v/v). The solution was evaporated under a stream of helium at 110 °C by applying conventional heating and further dried by azeotropic distillation using MeCN (1 mL) at a temperature of 110 °C. A solution of 2-bromoethyl triflate (5 μL, IsoSciences, Pennsylvania, USA) in o-dichlorobenzene (0.7 mL) was then added to the dried [^{18}F]F$^-$/K_2CO_3/kryptofix complex. The resulting [^{18}F]fluoroethyl bromide was then distilled at 120 °C with a helium flow (3−4 mL/min) and bubbled into a second reaction vial containing the precursor **33** (0.2 mg) and a small amount of Cs_2CO_3 (1−3 mg) in anhydrous DMF (0.2 mL). After distillation of a sufficient amount of radioactivity into the precursor solution, the reaction vial was closed and heated at 90 °C for 15 min. Next, the crude mixture was diluted with water (1.4 mL) and injected onto the HPLC system consisting of a semipreparative XBridge column (C_{18}, 5 μm, 4.6 mm × 150 mm; Waters) that was eluted with a mixture of 0.01 M NaH_2PO_4 buffer pH 2.2 and EtOH (90:10 v/v) at a flow rate of 1 mL/min. UV detection of the HPLC eluate was performed at 254 nm. The radiolabeled product [^{18}F]**3** was collected after 16 min. (The undesired isomer [^{18}F]**34** eluted after 23 min). The purified tracer was diluted with a basic phosphate buffer to obtain an ethanol concentration <5% and a pH in the range 5−8 and the solution was sterile filtered through a 0.22 μm membrane filter (Millex-GV, Millipore). The purity of the radiotracer was analyzed using an analytical HPLC system consisting of an XBridge column (C_{18}, 3.5 μm, 3 mm × 100 mm; Waters) eluted with a mixture of 0.01 M NaH_2PO_4 buffer pH 2.2 and MeCN (90:10 v/v) at a flow rate of 0.8 mL/min (Rt = 12.3 min). [^{18}F]**3** was synthesized in 45% radiochemical yield (relative to starting radioactivity of [^{18}F]fluoroethylbromide, decay corrected, n = 1). The radiochemical purity as examined using the above-described analytical HPLC system was >98%, and the specific radioactivity was 66 GBq/μmol at EOS.

*Method B Starting from Precursor Compound **35a** and [^{18}F]-Fluoride.* To a solution of **35a** (5 mg, 12 μmol) in DCM (1 mL) was added pyridine (11 μL, 136 μmol), and this solution was stirred at 0 °C. Methanesulfonic anhydride (16.5 mg, 95 μmol) was then added, and stirring was continued for 4 h at 0 °C, after which the solvent was evaporated by flushing with nitrogen. The crude mixture was redissolved in MeOH (0.5 mL), diluted with water (4.5 mL), and purified by solid phase extraction (C_{18} SepPak (Waters, Milford, MA, USA)). HPLC analysis was performed to examine the conversion of the hydroxyl-precursor **35a** into its O-mesyl derivative using an XTerra RP C_{18} column (5 μm, 4.6 mm × 250 mm; Waters) eluted with gradient mixtures consisting of water and MeCN (0 min: 95:5 v/v, 25 min: 10:90 v/v, 30 min: 10:90 v/v) at a flow rate of 1 mL/min. The analysis showed that the conversion rate was >95% (n = 11). Residual water was removed by azeotropic distillation with MeCN, and the mixture was dried overnight in the vacuum oven at rt. On the day of the radiolabeling experiment, (usually the next day), the reaction product was dissolved in anhydrous DMF (1.5 mL) and used (0.3 mL) for direct nucleophilic radiofluorination. The O-mesyl derivative was added to the dried [^{18}F]F$^-$/K_2CO_3/Kryptofix 222 complex, produced as described above, with the only difference that the [^{18}F]fluoride was eluted from the anion exchange cartridge using a mixture of MeCN (0.3 mL) and Kryptofix 222/K_2CO_3 solution (0.45 mL) instead of pure Kryptofix 222/K_2CO_3 solution (0.75 mL). The nucleophilic substitution reaction was carried out by conventional heating at 90 °C for 15 min. Next, the crude mixture was diluted with water (1.4 mL) and injected onto the HPLC system consisting of a semipreparative XBridge column (C_{18}, 5 μm, 4.6 mm × 150 mm; Waters) that was eluted with a mixture of 0.05 M NaOAc buffer pH 5.5 and EtOH (65:35 v/v) at a flow rate of 1 mL/min. UV detection of the HPLC eluate was performed at 254 nm. The radiolabeled product [^{18}F]**3** was collected after about 27 min. The collected peak corresponding to [^{18}F]**3** was then diluted with saline (Mini Plasco, Braun, Melsungen, Germany) to obtain a final EtOH concentration of <10%, and the solution was sterile filtered through a 0.22 μm membrane filter (Millex-GV, Millipore). The purity of the radiotracer was analyzed using an analytical HPLC system consisting of an XBridge column (C_{18}, 3.5 μm, 3 mm × 100 mm; Waters) eluted with a mixture of 0.05 M NaOAc buffer pH 5.5 and MeCN (65:35 v/v) at a flow rate of 0.8 mL/min (Rt = 5.4 min). UV detection of the HPLC eluate was performed at 254 nm. [^{18}F]**3** was synthesized in 17% radiochemical yield (relative to starting radioactivity [^{18}F]F$^-$, decay corrected, n = 8). The radiochemical purity as examined using the above-described analytical HPLC system was >97%, and the average specific radioactivity was found to be 167 GBq/μmol at EOS (n = 8).

*2-[[4-[1-(2-Fluoroethyl)-4-(4-pyridinyl)-1H-pyrazol-3-yl]phenoxy]-methyl]-5-[^{11}C]methoxy-pyridine ([^{11}C]**4**).* Carbon-11 was produced via a [^{14}N(p,α)^{11}C] nuclear reaction. The target gas, which was a mixture of N_2 (95%) and H_2 (5%), was irradiated using 18 -MeV protons at a beam current of 25 μA. The irradiation was done for about 30 min to yield [^{11}C]methane ([^{11}C]CH_4). The [^{11}C]CH_4 was then transferred to a home-built recirculation synthesis module and trapped on a Porapak column that was immersed in liquid nitrogen. After flushing with helium, the condensed [^{11}C]CH_4 was converted to the gaseous phase by bringing the Porapak loop to room temperature. This [^{11}C]CH_4 was then reacted with vaporous I_2 at 650 °C to convert it to [^{11}C]methyl iodide ([^{11}C]MeI). Subsequently, the [^{11}C]MeI was passed over a silver triflate column (6 mm × 50 mm) at 180 °C. The resulting [^{11}C]methyl triflate ([^{11}C]MeOTf) was bubbled with a flow of helium through a solution of the precursor **37** (0.2 mg) and Cs_2CO_3 (1−2 mg) in anhydrous DMF (0.2 mL). When the amount of radioactivity in the reaction vial had stabilized, the reaction mixture was left at rt for 3 min. The crude mixture was diluted with water (1 mL) and injected onto an HPLC system (XBridge C_{18}, 5 μm, 4.6 mm × 150 mm; Waters) eluted with a mixture of 0.05 M NaOAc (pH 5.5) and EtOH (65:35 v/v) at a flow rate of 1 mL/min. UV detection of the HPLC eluate was performed at 254 nm. The radiolabeled product [^{11}C]**4** was collected after 16 min. The collected peak corresponding to the desired radioligand was then diluted with saline (Mini Plasco, Braun, Melsungen, Germany) to obtain a final EtOH concentration of 10%, and the solution was sterile filtered through 0.22 μm membrane filter (Millex-GV, Millipore). Quality control was performed on an analytical HPLC system consisting of an XBridge C_{18}

3.5 μm column (3 mm × 100 mm; Waters) eluted with a mixture of 0.05 M NaOAc buffer (pH 5.5) and MeCN (70:30 v/v) at a flow rate of 0.8 mL/min (Rt = 7 min). UV detection was performed at 254 nm. [^{11}C]**4** was synthesized with a decay corrected radiochemical yield of <15% (relative to starting radioactivity of [^{11}C]MeOTf, n = 8) and with a radiochemical purity >99%.

*2-[[4-[1-(2-[^{18}F]Fluoroethyl)-4-(4-pyridinyl)-1H-pyrazol-3-yl]phenoxy]-methyl]-5-methoxy-pyridine ([^{18}F]**4**).* Compound **40a** was converted into its corresponding *O*-mesyl derivative as described for derivative **35a** and was then dissolved in anhydrous DMF (~0.6 mg in 0.3 mL of DMF). This solution was added to the dried [^{18}F]F^-/K_2CO_3/Kryptofix 222 complex, produced as described for [^{18}F]**3**, and the nucleophilic substitution reaction was carried out by conventional heating at 90 °C for 15 min. Next, the crude mixture was diluted with water (1.4 mL) and injected onto an HPLC system consisting of a semipreparative XBridge column (C_{18}, 5 μm, 4.6 mm × 150 mm; Waters) eluted with a mixture of 0.05 M NaOAc buffer pH 5.5 and EtOH (70:30 v/v) at a flow rate of 1 mL/min. UV detection of the HPLC eluate was performed at 254 nm. The radiolabeled product [^{18}F]**4** was collected after 36 min. The purified tracer was diluted with saline (Mini Plasco, Braun, Melsungen, Germany) to obtain an EtOH concentration of <10% and was sterile filtered through a 0.22 μm membrane filter (Millex-GV, Millipore). The purity of the radiotracer was analyzed using an analytical HPLC system consisting of an XBridge column (C_{18}, 3.5 μm, 3 mm × 100 mm; Waters) eluted with a mixture of 0.05 M NaOAc buffer pH 5.5 and MeCN (70:30 v/v) at a flow rate of 0.8 mL/min (Rt = 7.2 min). UV detection of the HPLC eluate was performed at 254 nm. [^{18}F]**4** was synthesized with a decay corrected radiochemical yield of 18% (relative to starting radioactivity of [^{18}F]F^-, n = 3). The radiochemical purity as examined using the above-described analytical HPLC system was >99%, and the average specific radioactivity was found to be 141 GBq/μmol at EOS (n = 3).

In Vitro Assay. Rat recombinant PDE10A (rPDE10A) was expressed in Sf9 cells using a recombinant rPDE10A baculovirus construct. Cells were harvested after 48 h of infection, and the rPDE10A protein was purified by metal chelate chromatography on Ni-sepharose 6FF. Tested compounds were dissolved and diluted in 100% DMSO to a concentration 100-fold of the final concentration in the assay. Compound dilutions (0.4 μL) were added in 384-well plates to 20 μL of incubation buffer (50 mM Tris pH 7.8, 8.3 mM $MgCl_2$, 1.7 mM EGTA). Then 10 μL of rPDE10A enzyme in incubation buffer was added and the reaction was started by addition of 10 μL of substrate to a final concentration of 60 nM cAMP and 0.008 μCi [^{3}H]cAMP. The reaction was incubated for 60 min at rt. After incubation, the reaction was stopped with 20 μL of 17.8 mg/mL PDE SPA beads. After sedimentation of the beads during 30 min, the radioactivity was measured in a Perkin-Elmer Topcount scintillation counter and results were expressed as cpm. For blank values, the enzyme was omitted from the reaction and replaced by incubation buffer. Control values were obtained by addition of a final concentration of 1% DMSO instead of compound. A best fit curve was fitted by a minimum sum of squares method to the plot of % of control value subtracted with blank value versus compound concentration, and a pIC_{50} value was derived from this curve.

In Vivo Occupancy Protocol. Rats were treated by subcutaneous administration of vehicle or different dosages of selective PDE10A inhibitors (n = 3 per dose) and after 30 min [^{3}H]MP-10 (10 μCi) was injected intravenously. Rats were sacrificed 30 min after the tracer injection and their brains dissected and frozen. Then 20 μm thick coronal sections were cut using a cryostat and collected on glass slides. Brain sections were loaded in a β-imager for 8 h. The specific binding was determined as the difference between [^{3}H]MP-10 binding quantified in the striatum (a brain area showing a high density of PDE10A) and in the cortex (a brain area where PDE10A is virtually absent). Occupancy was calculated as the inhibition of specific [^{3}H]MP-10 binding in drug-treated animals relative to vehicle-treated animals. For the determination of ED_{50}s (dose occupying 50% of PDE10A), the percentage of PDE10A occupancy was plotted against dosage, and the sigmoidal log dose−effect curve of best fit was calculated by nonlinear regression analysis, using the GraphPad Prism program.

Biodistribution Studies. Biodistribution studies were carried out in healthy male Wistar rats (body weight 200−500 g) at 2, 30, and 60 min post injection (pi) (n = 3 per time point). Rats were injected with about 1.1 MBq of the tracer via a tail vein under anesthesia (2.5% isoflurane in O_2 at 1 L/min flow rate) and sacrificed by decapitation at above specified time points. Blood and major organs were collected in tared tubes and weighed. The radioactivity in blood, organs, and other body parts was counted using an automated γ counter. For calculation of total radioactivity in blood, blood mass was assumed to be 7% of the body mass. Quantification of radioactivity measurements in samples of biodistribution studies was done using an automated γ counter equipped with a 3-in. NaI(Tl) well crystal coupled to a multichannel analyzer (Wallac 1480 Wizard, Wallac, Turku, Finland). All animal experiments were conducted with the approval of the institutional ethical committee for conduct of experiments on animals.

■ ASSOCIATED CONTENT

Supporting Information. The elemental analysis data of the final compounds that were isolated as succinic acid salts, the description of the different methods used for the LCMS-characterization of the compounds described in this manuscript, and the CEREP screening reports for compounds **3** and **4**. This material is available free of charge via the Internet at http://pubs.acs.org.

■ AUTHOR INFORMATION

Corresponding Author

*Phone: + 34 925 245 780. Fax: + 34 925 245 771. E-mail: iandres@its.jnj.com.

■ ACKNOWLEDGMENT

We thank José Manuel Alonso, Luis Font, and Alberto Fontana of the Analysis & Purification Department in Toledo for their skillful assistance. We also thank Ivan Sannen and Julie Cornelis of the Laboratory for Radiopharmacy for their skillful help with the biodistribution studies.

■ ABBREVIATIONS USED

cAMP, 3′,5′-cyclic adenosine monophosphate; cGMP, 3′,5′-cyclic guanosine monophosphate; DCM, dichloromethane; DIAD, diisopropyl azodicarboxylate; DIPE, diisopropylethyl ether; EOS, end of synthesis; LDA, lithium diisopropylamide; MW, microwave heating; PDE, phosphodiesterase; PDE10A, phosphodiesterase subtype-10A; PET, positron emission tomography; pi, post injection; RCY, decay-corrected radiochemical yield; RP-HPLC, reversed phase-high performance liquid chromatography; Rt, retention time; rt, room temperature; SD, standard deviation; SUV, standardized uptake value; TFA, trifluoroacetic acid

■ REFERENCES

(1) Conti, M.; Beavo, J. Biochemistry and Physiology of Cyclic Nucleotide Phosphodiesterases: Essential Components in Cyclic Nucleotide Signaling. *Annu. Rev. Biochem.* **2007**, *76*, 481–511.

(2) Mennitti, F. S.; Faraci, W. S.; Schmidt, C. J. Phosphodiesterases in the CNS: Targets for Drug Development. *Nature Rev. Drug Discovery* **2006**, *5*, 660–669.

(3) (a) Loughney, K.; Snyder, P. B.; Uher, L.; Rosman, G. J.; Ferguson, K.; Florio, V. A. Isolation and Characterization of PDE10A, A Novel Human 3′,5′-Cyclic Nucleotide Phosphodiesterase. *Gene* **1999**, *234*, 109–117. (b) Soderling, S. H.; Bayuga, S. J.; Beavo, J. A. Isolation and Characterization of a Dual-Substrate Phosphodieasterase Gene Family: PDE10A. *Proc. Natl. Acad. Sci. U.S.A.* **1999**, *96*, 7071–7076. (c) Fujishige, K.; Kotera, J.; Michibata, H.; Yuasa, K.; Takebayushi, S.; Okumura, K.; Omori, K. Cloning and Characterization of a Novel Human Phosphodiesterase that Hydrolyzes Both cAMP and cGMP (PDE10A). *J. Biol. Chem.* **1999**, *274*, 18438–18445.

(4) Fujishige, K.; Kotera, J.; Omori, K. Striatum- and testis-specific phosphodiesterase PDE10A. Isolation and characterization of a rat PDE10A. *Eur. J. Biochem.* **1999**, *266*, 1118–1127.

(5) Seeger, T. F.; Bartlett, B.; Coskran, T. M.; Culp, J. S.; James, L. C.; Krull, D. L.; Lanfear, J.; Ryan, A. M.; Schmidt, C. J.; Strick, C. A.; Varghese, A. H.; Williams, R. D.; Wylie, P. G.; Menniti, F. S. Immunohistochemical Localization of PDE10A in the Rat Brain. *Brain Res.* **2003**, *985*, 113–126.

(6) Halene, T. B.; Siegel, S. J. PDE10 Inhibitors in Psychiatry—Future Options for Dementia, Depression and Schizophrenia? *Drug Discovery Today* **2007**, *12*, 870–878

(7) Passchier, J.; Gee, A.; Willemsen, A.; Vaalburg, W.; van Waarde, A. Measuring drug-related receptor occupancy with positron emission tomography. *Methods* **2002**, *27*, 278–286.

(8) Wong, D. F.; Tauscher, J.; Gründer, G. The role of imaging in proof of concept for CNS drug discovery and development. *Neuropsychopharmacology* **2009**, *34*, 187–203.

(9) Tu, Z.; Xu, J.; Jones, L. A.; Li, S.; Mach, R. H. Carbon-11 Labeled Papaverine as a PET Tracer for Imaging PDE10A: Radiosynthesis, In Vitro and In Vivo Evaluation. *Nucl. Med. Biol.* **2010**, *37*, 509–516.

(10) Celen, S.; Koole, M.; De Angelis, M.; Sannen, I.; Chitneni, S. K.; Alcazar, J.; Dedeurwaerdere, S.; Moechars, D.; Schmidt, M.; Verbruggen, A.; Langlois, X.; Van Laere, K.; Andrés, J. I.; Bormans, G. Preclinical Evaluation of ^{18}F-JNJ41510417 as a Radioligand for PET Imaging of Phosphodiesterase-10A in the Brain. *J. Nucl. Med.* **2010**, *51*, 1584–1591.

(11) Chappie, T. A.; Humphrey, J. M.; Allen, M. P.; Estep, K. G.; Fox, C. B.; Lebel, L. A.; Liras, S.; Marr, E. S.; Menniti, F. S.; Pandit, J.; Schmidt, C. J.; Tu, M.; Williams, R. D.; Yang, F. V. Discovery of a Series of 6,7-Dimethoxy-4-pyrrolidylquinazoline PDE10A Inhibitors. *J. Med. Chem.* **2007**, *50*, 182–185.

(12) Pike, V. W. PET Radiotracers: Crossing the Blood—Brain Barrier and Surviving Metabolism. *Trends Pharmacol. Sci.* **2009**, *30*, 431–440.

(13) Laruelle, M.; Slifstein, M.; Huang, Y. Relationships between radiotracer properties and image quality in molecular imaging of the brain with positron emission tomography. *Mol. Imaging Biol.* **2003**, *5*, 363–375.

(14) Ooms, M.; Celen, S.; Verbruggen, A.; Van Laere, K.; Bormans, G. Synthesis and preliminary biological evaluation of [^{11}C]-MP10 and its regioisomer as potential radioligands for positron emission tomography imaging of phosphodieasterase-10A in the brain. *Eur. J. Nucl. Med. Mol. Imaging* **2010**, *37*, S206–S206.

(15) Tu, Z.; Fan, J.; Li, S.; Jones, L. A.; Cui, J.; Padakanti, P. K.; Xu, J.; Zeng, D.; Shoghi, K. I.; Perlmutter, J. S.; Mach, R. H. Radiosynthesis and in vivo evaluation of [^{11}C]MP-10 as a PET probe for imaging PDE10A in rodent and nonhuman primate brain. *Bioorg. Med. Chem.* **2011**, *19*, 1666–1673.

(16) Verhoest, P. R.; Chapin, D. S.; Corman, M.; Fonseca, K.; Harms, J. F.; Hou, X.; Marr, E. S.; Menniti, F. S.; Nelson, F.; O'Connor, R.; Pandit, J.; Proulx-LaFrance, C.; Schmidt, A. W.; Schmidt, C. J.; Suiciak, J. A.; Liras, S. Discovery of a Novel Class of Phosphodiesterase 10A Inhibitors and Identification of Clinical Candidate 2-[4-(1-Methyl-4-pyridin-4-yl-1*H*-pyrazol-3-yl)-phenoxymethyl]-quinoline (PF-2545920) for the Treatment of Schizophrenia. *J. Med. Chem.* **2009**, *52*, 5188–5196.

(17) Verhoest, P. R.; Helal, C. J.; Hoover, D. J.; Humphrey, J. M. Heteroaromatic Quinoline Compounds. PCT Int. Appl. WO200-6072828, 2006.

(18) Chen, Q.-Y. Trifluoromethylation of organic halides with difluorocarbene precursors. *J. Fluorine Chem.* **1995**, *72*, 241–246.

(19) Zhang, M.-R.; Tsuchiyama, A.; Haradahira, T.; Yoshida, Y.; Furutsuka, K.; Suzuki, K. Development of an automated system for synthesizing ^{18}F-labeled compounds using [^{18}F]fluoroethyl bromide as a synthetic precursor. *Appl. Radiat. Isot.* **2002**, *48*, 335–342.

(20) Behr, J.-B.; Gourlain, T.; Helimi, A.; Guillerm, G. Design, Synthesis and Biological Evaluation of Hetaryl-Nucleoside Derivatives as Inhibitors of Chitin Synthase. *Bioorg. Med. Chem. Lett.* **2003**, *13*, 1713–1716.

(21) clogP values were calculated from Daylight software and Biobyte, Inc. of Claremont, CA.

(22) Waterhouse, R. N. Determination of lipophilicity and its use as a predictor of blood—brain barrier penetration of molecular imaging agents. *Mol. Imaging Biol.* **2003**, *5*, 376–389.

(23) Langlois, X.; Lenaerts, I.; Van der Linden, I.; Lavreysen, H.; Vanhoof, G.; Vliegen, M.; Alcazar J.; De Angelis, M.; Andres, J. I. Use of the radioligand [^{3}H]MP-10 to map PDE10A expression and measure PDE10A occupancy in rat brain. *Soc. Neurosci. Annu. Meet.* **2009**, 646.26.

(24) Method for identification of main metabolites: the test compounds were incubated with human and rat liver microsomes, at 0.4% final solvent concentration (0.16% DMSO and 0.24% MeCN). The study was conducted to identify the main metabolites formed after 0 min (control) and 60 min incubation time in presence of NADPH generating system at 37 °C. Test concentration of the compound was 5 μM. Samples were compared to the control incubations in which compound was added at termination. Data were acquired on a Waters UPLC/QToF Premier mass spectrometer using a 10 min generic UPLC method and a generic MSe method. Complementary MS/MS experiments were performed when necessary. An Acquity UPLC C18 (2.1 mm × 100 mm, 1.8 μm) column was used. Interpretation of data was performed with Waters Metabolynx software.

(25) Hatanaka, M.; Takahashi, K.; Nakamura, S.; Mashino, T. Preparation and antioxidant activity of α-pyridoin and its derivatives. *Bioorg. Med. Chem.* **2005**, *13*, 6763–6770.

(26) Mizuno, Y.; Endo, T.; Nakamura, T. Preparation of 2-pyridyl-, 2-quinolyl-, and 1-isoquinolyldiazomethane *N*-oxides and alkylation of acidic hydroxylic functions. *J. Org. Chem.* **1975**, *40*, 1391–1395.

(27) Ashimori, A.; Ono, T.; Uchida, T.; Ohtaki, Y.; Fukaya, C.; Watanabe, M.; Yokoyama, K. Synthesis and hypotensive activity of 4-(substituted pyridyl)-1,4-dihydropyridine derivatives. *Chem. Pharm. Bull.* **1990**, *38*, 2446–58.

(28) Kasibhatla, S. R.; Hong, K.; Biamonte, M. A.; Busch, D. J.; Karjian, P. L.; Sensintaffar, J. L.; Kamal, A.; Lough, R. E.; Brekken, J.; Lundgren, K.; Grecko, R.; Timony, G. A.; Ran, Y.; Mansfield, R.; Fritz, L. C.; Ulm, E.; Burrows, F. J.; Boehm, M. F. Rationally Designed High-Affinity 2-Amino-6-halopurine Heat Shock Protein 90 Inhibitors That Exhibit Potent Antitumor Activity. *J. Med. Chem.* **2007**, *50*, 2767–2778.